Is the Absorption of Anaesthetic Agents Non Linear?

Johan Daniel Steyn
Student Number: 8502331

Submitted in partial fulfilment of the requirements of the degree PhD, in the Faculty of Medicine, University of Pretoria.

Promoter: Professor JM Hugo, Department of Anaesthesiology University of Pretoria
Co promoter: Professor C Steinmann, Department of Physiology University of Pretoria

Acknowledgements

Prof. JM Hugo: Head of Department of Anaesthesiology and Promoter

Prof. C Steinmann: Co Promoter

Dr C Becker: Biostatistician, University of Pretoria

Dr F Smith: Anaesthesiologist, Principle Specialist, Department of Anaesthesiology, University of Pretoria

Dr W Pearce: Senior Registrar, Department of Anaesthesiology, University of Pretoria

Summary

Knowledge of the absorption of inhalation anaesthetic agents is essential if one is to safely administer them. Despite many years of research in linear science, no model has been described that can reliably predict inhalation agent uptake. To date no published investigation has looked for non-linearity in the absorption process. The aim if this research project was to determine if the absorption of anaesthetic agents is non-linear, using isoflurane and enflurane as examples.

To detect non-linearity, four conditions must be met:
Sensitivity to initial conditions,
Fractal Dimension of the attractor,
Invariant probability distribution of the attractor, and
Detection of an underlying dynamical process.

Ten measured time series for both isoflurane and enflurane absorption were measured. These were then compared with ten noise signals, with similar standard deviations, means and number of points in the series.

Calculated Lyapunov exponents tested sensitivity to initial conditions. The dimension of the attractor was calculated using the following statistics, each giving an approximation of the fractal dimension. Approximate entropy, information entropy, correlation dimension and fractal dimension (box counting method). The Invariant probability distribution of the attractor was tested for using non-linear forecasting. Detection of an underlying dynamical process was determined by the method of surrogate data.

Each of the four conditions required have been met with statistical significance ($p< 0.05$) and acceptable statistical power (>0.8). It is therefore concluded that the absorption of both isoflurane and enflurane are non-linear processes. The implications and implementations in anaesthesia practice are discussed.

Opsomming

'n Deeglike kennis van die opname van narkose dampe is nodig om die toediening daarvan veilig te maak. Ten spyte van etlike jare van navorsing, is geen liniêre model beskryf wat die opname van dampe akkuraat voorspel nie. Geen publikasie het tot op hede die hipotese van nie-liniêre absorpsie van narkosedampe ondersoek nie. Die doel van die navorsingsprojek is om die moontlikheid dat die opname van narkose dampe nie-liniêr is te ondersoek, met gebruik van isofluraan en enfluraan as voorbeelde.

Om vir nie lineariteit te toets, moet daar aan die volgende vereistes voldoen word:
Sensitiwiteit vir aanvanklike omstandighede,
Fraktale dimensie van die attraktor,
Invariante waarskynlikheids verspreiding van die attraktor, en die Identifisering van 'n onderliggende dinamiese proses.

Tien gemete tydreekse is vir beide isofluraan- en enfluraan-absorpsie afsonderlik bepaal. Dié is vergelyk met tien ruis-tydreekse met vergelykbare standaardafwykings, gemiddelde waardes en aantal datapunte in elke betrokke reeks.

Berekende Lyapunov eksponente is gebruik om te toets vir sensitiwiteit vir aanvanklike omstandighede. Die attraktor-dimensie is gemeet met die volgende statistiese metodes, waar elkeen 'n beraming gee van die fraktale dimensie. Benaderde entropie, inligtings-entropie, korrelasie-dimensie en fraktale-dimensie (blok-tel-metode). Die invariant waarskynikheids-verspreiding van die attraktor is bepaal deur nie-liniêrevoorspelling. Identifisering van 'n onderliggende dinamiese proses is gedoen volgens die metode van surrogaat-data.

Daar is aan al die vereistes van statistiese betekenis voldoen ($p<0.05$) en aanvaarbare statistiese krag (>0.8). Met analise van beskikbare data is die

gevolgtrekking dat die opname van narkose-dampe nie-liniêr geskied. Die implikasies en toepaslikheid in narkose praktykvoering word bespreek.

Declaration

I, Johan Daniel Steyn do hereby solemnly declare that this is my own original work, and that it has not been submitted to any other university for degree purposes.

Signed: Johan Steyn

Date: 21/02/2003

TABLE OF CONTENTS

LIST OF TABLES

LIST OF FIGURES

1 Introduction

Knowledge of the absorption of inhalation anaesthetic agents is essential if one is to safely administer them. Severinghaus was the first to systematically study inhalation agent absorption, and his investigations resulted in the "square root of time model"[1, 2] . As the possibility of computer-assisted anaesthesia administration becomes a reality, interest in this fundamental aspect of anaesthesia has continued to remain intense. Despite many years of research in linear science, no model has been described that can reliably predict inhalation agent uptake.

In a recent essay in The Lancet, Ary L Goldberger[3] states that, "Clinicians are increasingly aware of the remarkable upsurge of interest in non-linear dynamics, the branch of sciences widely referred to as chaos theory. The extent to which chaos relates to physiological dynamics is being investigated and is controversial. Chaos theory also holds promise for the elucidation of major problems in contemporary physiology and molecular biology."

A literature study was conducted to see if the possibility that the absorption of inhalation agents was a non-linear process had been investigated. Not a single reference could be found.

The aim if this research project is to determine if the absorption of anaesthetic agents is non-linear, using isoflurane and enflurane as examples.

---

[1] Severinghaus J.W. The Rate Of Uptake Of Nitrous Oxide In Man. Journal Of Clinical Investigation 1954:33;1183-1189.

[2] Lowe H.J.,Ernst E.A. The Quantitative Practice Of Anaesthesia - Use Of The Closed Circuit. Baltimore: Williams And Wilkins, 1981.

[3] Goldberger A.L. Non-Linear Dynamics For Clinicians: Chaos Theory, Fractals And Complexity At The Bedside. The Lancet 1996:347;1312-1314.

2 Literature Study

2.1 Linear Models Described in the Literature

2.1.1 The square root of time model

This model was described by Severinghaus and refined by Lowe[1, 2]. The uptake of a potent inhaled anaesthetic is said to be predicted by the square root of time. This concept has been widely accepted during the past forty years, despite its shortcomings.

A "unit dose" is taken up by the body during the first minute and during each subsequent time interval (3 min, 5 min, 7 min, 9 min, 11 min, etc). In addition, a prime dose is required to saturate the circuit, the functional residual capacity, and the arterial delivery system. The addition of the prime and unit doses yields the cumulative dose. The doses are calculated using equations incorporating the patient's estimated cardiac output, anaesthetic agent minimum alveolar concentration (MAC), molecular weight, and blood/gas partition coefficient of the inhalation agent in use.

Unit dose (Liters of vapor) = 2 x fraction of minimum alveolar concentration being delivered x minimum alveolar concentration x blood gas partition coefficient x cardiac output.

Prime dose (Liters of vapor)= Unit dose (liters of vapor) = 2 x fraction of minimum alveolar concentration being delivered x minimum alveolar concentration x blood gas partition coefficient x cardiac output + circuit and functional residual capacity volume x fraction of minimum alveolar concentration x minimum alveolar concentration.

Cumulative dose (Liters of vapor)=prime dose + unit dosex $\sqrt{}$time in minutes.

The cardiac output is estimated using the formula of DeBrodie:

Cardiac output = 0.2 x mass$^{3/4}$ (liters per minute)^{2}.

This model was derived with data obtained form five (5) patients, using a narcotest gas analyzer. This type of apparatus calculates the concentration of inhalation agent based on its absorbtion by silicone. It was popular in the 1950's.[5]

2.1.2 The relationship between anaesthetic uptake and cardiac output

Watt et al.[3] investigated the relationship between cardiac output and anaesthetic uptake. They predicted that the continuous measurement of uptake of a volatile anaesthetic agent during inhalation anesthesia would prove to be a sensitive guide to trends in cardiac output. This hypothesis was tested by comparing the rate of uptake of enflurane at a constant end expired concentration of 1% (in reality the uptake was not measured, only the anaesthetic agent requirement to maintain a 1% end tidal concentration), with repeated thermodilution cardiac output measurements in patients undergoing cardiac surgery. A closed breathing system using a computer controlled liquid enflurane injection system was used to maintain the constant end tidal concentrations. In all 266 cardiac output measurements were made before cardiopulmonary bypass. No combined statistics are presented, but coefficients of determination (r^2) ranging from 0.16 to 0.42 were reported. The conclusion reached by the authors was that a qualitative but not quantitative relationship was demonstrated, and that they were unable to derive a clinically useful quantitative measure of cardiac output from the rate of the enflurane uptake using a computer controlled system[3].

These findings refute the square root of time model, where the only patient dependent variable is an estimation of the cardiac output.

2.1.3 Re-evaluations of the Square Root Of Time Model

Recently, the square root of time model has been subject to numerous re-evaluations[4,5,6,7,8]. None of these investigators were able to validate the model.

2.1.3.1 Couto Da Silva et al

These authors[8] studied the square root of time model in a quantitative way to test its clinical use, particularly for developing countries. The technique of intermittent injection into a closed circuit was used. The concentrations of inhalation agent were measured, but blinded from the investigator, and the systolic blood pressure was used as an end point. The objective was to maintain a value within 20% of pre-induction values. The prescribed doses were adhered to, but after the first two, they were adjusted according to the systolic blood pressures. The mean doses found necessary for each anaesthetic were within 33% of those calculated to produce 1.3 minimum alveolar concentration, however, the end-tidal concentrations stabilized at levels of 0.97 minimum alveolar concentration for halothane, 0.43 minimum alveolar concentration for enflurane and 0.77 minimum alveolar concentration for isoflurane. This represents a range of 33% to 74% of predicted values. They concluded that the Lowe intermittent-injection square root of time method of closed circuit anaesthesia provides a basis for simple, economic anaesthesia, but that the uptake of anaesthetic agents declined more slowly than predicted.

2.1.3.2 Hendrickx et al

Hendrickx et al[5]investigated the uptake of desflurane and isoflurane during closed-circuit anaesthesia using liquid injection techniques, to see if patient characteristics predict desflurane and isoflurane uptake, and, if the mode of ventilation had any effect on uptake. The investigation was initiated by the recent clinical observations on the uptake of inhaled anesthetics which conflict the square root of time model[9,10,7,6,11], where some authors have suggested that the uptake of anaesthetic gases is fairly constant during the first 60 to 100 minutes[11] and the inability to correlate isoflurane and enflurane uptake with patient characteristics[7,6].

For this study the cumulative dose and end expired concentrations of anaesthetic gases were recorded over time at one minute intervals. Individual uptake curves were fitted when a 1.3 * minimum alveolar

concentration values were obtained. The cumulative doses after 4, 15, 30, 45 and 60 minutes as well as the variables of the fitted curves of each individual were correlated with patient characteristics. The desflurane and isoflurane uptake was compared with the square root of time model. The uptake during controlled and spontaneous ventilation were compared to determine the effects of the mode of ventilation of the uptake of anaesthetic agents.

Within each group, there was interindividual variability in the uptake at all times, with a coefficient of variation of 8% to 20%. The cumulative dose versus time data, did not correlate with any of the patient characteristics, neither did the cumulative doses as 4, 15, 30, 45 and 60 minutes. No significant difference was found between spontaneous and controlled ventilation. The square root of time model was found to overestimate the uptake, especially during the first part of the procedure.

			R^2 BETWEEN SLOPE AND PATIENT CHARACTERISTICS				
Agent	Slope of linearly fittted curve	Range of slope	Age	Height	Weight	$Weight^{3/4}$	Body surface area
Desflurane (Spontaneous)	0.22	0.174-0.313	0.281	0.306	0.689	0.674	0.635
Desflurane (Controlled)	0.22	0.191-0.246	0.145	0.122	0.212	0.206	0.126
Isoflurane (Spontaneous)	0.1	0.077-0.125	0.166	0.470	0.274	0.273	0.453
Isoflurane (Controlled)	0.11	0.088-0.131	0.004	0.027	0.002	0.002	0.006

Table 2-1 Anaesthetic Uptake As Represented By The Slope Of The Linearly Fitted Curve And Coefficient Of Determination (R^2) Between The Slope And Patient Characteristics. (After Hendrickx Et Al[5])

Inter-individual variation in uptake in this study was observed, with poor correlation between uptake and patient characteristics. These results are similar to others recently published[9,7,12].

2.1.3.3 Bengston et al

Bengston et al[4] undertook a study to investigate uptake rates of enflurane and isoflurane during spontaneous and controlled ventilation. No significant difference in uptake was found between spontaneous and controlled ventilation, regardless of the agent used. They conclude, "In the present study, the anaesthetic uptake rates of the square root of time concept

could not be confirmed." If unit doses according to Lowe's formula were to be injected in a closed circuit system, the amount of liquid anaesthetic would not correspond to the patient's uptake rate.

2.1.4 The System model for closed circuit inhalation anaesthesia

The System model for closed circuit inhalation anaesthesia[13] and other models have recently been described [6,7,13], but only the Systematic Model has been subject to systematic performance evaluation. The purposes of constructing this model were to construct a model that simulates the uptake and distribution of a single inhaled anaesthetic agent during closed circuit anaesthesia and to extend the basic model to more elaborate models with additional features. The model does not assume a constant alveolar concentration, and therefore lends itself for validation by non-invasive measuring techniques such as respiratory mass spectometry[13].

The basic model for the uptake and distribution of a single inhaled anaesthetic agent depicts the body and the closed circuit as a system of 14 compartments. The anaesthetic is taken up from the lung-close circuit compartment and is then distributed to other tissue compartments: kidney, brain, heart, liver, muscle, connective tissue, and adipose tissue. The model derives from the subject's age, weight, height and gender the other physiologic variables including tissue volumes, blood volume, cardiac output, dead space, alveolar space and tidal volume. The data for the total blood volume, cardiac output, tissue volumes, tissue blood flow and partitian coefficients are derived from Lowe's data. The volume into which the anaesthetic agent is distributed in the lung not only includes the mid-inspiratory alveolar gas volume, i.e. the mid-inspiratory alveolar gas volume plus half the tidal volume, but also the lung tissue volume multiplied by its tissue-gas partitian coefficient. The functional residual capacity is calculated as a function of height, age, and gender with the aid of a regression equation for un-anaesthetized subjects in the sitting position. It was subsequently adapted for a supine, anaesthetized subject by a correction factor of 0.65.[13]

All blood is stored in pools, thus simulating the differences in circulation times that exist in the body. One fifth of the total blood volume is at arterial tension and is stored in the arterial pool. The rest of the blood is shared among the central venous pool and three venous pools associated with tissues and organs grouped into compartments, mainly based on perfusion.[13]

The basic model is intended to operate with controlled ventilation and does not take into account the concentration and second gas effects. Alveolar ventilation is the difference between total ventilation and dead space ventilation. The basic model has two versions: these differ in the size of their peripheral shunt: the shunt is 0 and 16% of the cardiac output for Version A and B respectively[13].

A liquid anaesthetic agent injected directly into the closed system is assumed to mix uniformly after vaporization with the contents of the anaesthetic system as to behave as an ideal gas. A bolus injection of liquid anaesthetic was simulated by adding anaesthetic vapor to the closed system over a period of 60 seconds[13].

The model has some important unique features: it includes the breathing system and does not avoid the complexity of the closed system[13]. One must note that it does not consider the alveolar membrane as a barrier[11] as the lung tissue volume is included in the lung compartment volume[13]. Unlike earlier closed circuit anaesthesia models it does not assume constant arterial concentration or zero calculation time. It is written with the aid of a special purpose simulation language developed at the University of Technology (The Netherlands)[13].

Different versions of the model were subject to quantified predictive performance evaluations by comparison of the predicted and measured alveolar concentrations profiles in 53 patients. Each concentration was measured by mass spectrometry and was compared to four predicted concentrations calculated by the four computer simulations (one per version of the model). For each patient, the authors calculated the root mean

squared error, bias, and the scatter of the prediction errors. Liquid halothane[14] was used in this performance evaluation. The version showing the best overall performance showed a root mean square error of 19.6±7.2% (mean±standard deviation), a bias of 0.5±15.9% and a scatter of 13.2±3.5%. The range of the results for all the models was: root mean square error 19.6 to 25.3%, the bias .48 to 13.57% and the scatter 13.18 to 15.92%[14].

The model incorporating non-pulmonary elimination and age adjusted partitian coefficients proved to be the most accurate and was said to be sufficiently reliable and accurate to represent halothane closed circuit anaesthesia[14].

The same model was evaluated in a performance evaluation quantifying the total variability and within patient variability, but between repeat anaesthetics variability[15]. Fourteen patients were studied who received closed circuit enflurane anaesthesia on two occasions. The end tidal concentrations measured and those predicted served to calculate the predictive performance measures of the model. The overall results were: the root mean squared error 15±7%, bias 0±14% and scatter 9±3%. The within the patient standard deviations were smaller for the root mean squared error (4%) and bias (10%), but not for scatter (3%)[15].

The estimated variance resulting from within patient variance was 90%. The authors conclude that the performance measures were partly dependent on the patient. There was no association between the personal performance measures and age, sex, body weight, body surface area or body mass index. These findings lead the authors to conclude, "Additional, yet unknown factors may contribute in a significant extend to an individuals pharmacokinetic response"[15].

2.1.5 Simple linear regression models

2.1.5.1 Lockwood et al

Two almost identical studies[6,7] investigating the uptake of desflurane and isoflurane respectively were published by these authors. Both studies

report linear regression fit equations using the best least squares fit method. A bi-exponential equation was reported for isoflurane and a tri-exponential one for desflurane. However, no coefficient of determination is reported for either equation, and only one study[7] reported a cumulative mean and standard deviation for the dose of isoflurane given. Perturbations from the equation were assumed to reflect changes in cardiac output. Due to lack of vital information, these results must be interpreted with caution.

2.2 Non linear dynamics and medicine

2.2.1 Non linear dynamics in general

The entire section 2.2.1 is taken from an article by JD Meiss of Boulder, Colorado[16].

2.2.1.1 What is non-linear?

In geometry, linearity refers to Euclidean objects: lines, planes, three dimensional space etc. these objects appear the same no matter how they are examined. A non-linear object, a sphere for example, looks different on different scales, when looked at closely enough it looks like a plane, and from far enough distance it looks like a point.

In algebra linearity is defined in terms of functions that have the property $f(x+y)=f(x)+f(y)$ and $f(ax)=af(x)$. Non-linear is defined as the negation of linear. This means that the result f may be out of proportion to the input x or y. The result may be more than linear or less than linear.

2.2.1.2 What is non-linear science?

Linearity is rather special and no model of a real system is truly linear. Some things are profitably studied as linear approximations to the real model.

Nonlinear systems have been shown to exhibit surprising and complex effects that would never be anticipated by a scientist trained only in linear techniques. While linear objects can be enumerated, nonlinear ones

are nonenumerable, and as of yet mostly unclassified. There is currently no general technique for telling whether a particular nonlinear system will exibit the complexity of chaos, or the simplicity of order. Thus as nonlinear science cannot be subdivided into proper subfields, it exists as a whole. Nonlinear science has applications to a variety of fields from mathematics, physics, biology and chemistry, engineering, economics and medicine. One of its most exciting aspects, is that it brings researchers from many disciplines together with a common language.

2.2.1.3 What is a dynamical system?

A dynamical system consists of an abstract phase space or state pace, whose coordinates describe the dynamical state at any instant, and a dynamical rule which specified the immediate future trend of all state variables, given only the present values of those same state variables. Mathematically, a dynamical system is described by an initial value problem.

Dynamical systems are determinestic if there is a unique consequent to every state, and stochastic or random if there is more than one consequent chosen from some probability distribution e.g. tossing a coin has two consequents with equal probability for each initial state.

2.2.1.4 What is phase space?

Phase space is the collection of possible states of a dynamical system. A phase space can be finite (limited number of states), countably finite (integer) or uncountalbly infinite (state variables are real numbers). Implicit in the notion is that a particular state in phase space specifies the system completely, all that we need to know about a system to have complete knowledge of its immediate future.

The path in phase space traced out by a solution of an initial value problem is called an orbit or trajectory of the dynamical system. If the state variables take real values in a continuum, the orbits or continuous time

system is a curve, while the orbit of a discrete system is a sequence of points.

2.2.1.5 What is chaos?

In mathematical terms, chaos is effectively unpredictable long time behavior arising in a deterministic dynamical system because of sensitivity to initial conditions. A deterministic dynamical system is perfectly predictable given perfect knowledge of the initial conditions.

For a dynamical system to be chaotic, it must have a large set of initial conditions, which are highly unstable. No matter how precisely you measure the initial conditions in these systems, your prediction of its subsequent motion goes radically wrong after a time. The key to long term unpredictability is a property known as sensitivity to (or sensitive dependence on) initial conditions. Typically, the predictability horizon grows only logarithmically with the precision of measurements. A chaotic system can be represented in phase space.

2.2.1.6 What are fractals?

A fractal as defined by Mandelbrot is a set with a fractional (non integer) dimension, and a self similar structure. The dimensions of properties measured are dependent on the scale of measurement. Self-similarity implies that measurement at a smaller scale will yield similar characteristics to those at a larger scale.

2.2.2 Non-linear Dynamics and Medicine

Clinicians are increasingly aware of the remarkable upsurge of interest in non-linear dynamics; the branch of science widely referred to as chaos theory[17]. Linear systems are well behaved. The magnitude of their responses is proportionate to the strength of the stimuli. These systems can be fully understood and predicted by dissecting out their components, and these subunits add up without surprises or anomalous behaviors. By contrast for non-linearity proportionality does not hold, neither can the

system be understood by analyzing their components individually. The reductionism strategy fails because the components of the non-linear system are coupled. Their non-linear coupling generates behaviors that defy explanation by traditional (linear) models such as self-sustained, periodic waves (e.g. ventricular tachycardia), abrupt changes (e.g. sudden onset of a seizure) and, possibly chaos[17].

One important class of abrupt, non-linear transition is called a bifurcation, which describes situations in which a very small increase or decrease in the value of some factor controlling the system causes it to change abruptly from one type of behavior to another. A common type of bifurcation is the sudden appearance of regular oscillations that alternate between two values. This dynamic may underlie various alternans patterns in cardiovascular dysfunction. A familiar example is the beat to beat alternation in QRS axis and amplitude seen in some cases of cardiac tamponade[18]. Many other examples of alternans in pertubated cardiac physiology have been described such as ST-T alternans preceding ventricular fibrillation, and pulsus alternans during heart failure[19].

The extent to which chaos relates to physiological dynamics is being investigated and is controversial[17]. At first, it was widely assumed that chaotic fluctuations were produced by pathological systems such as cardiac electrical activity during atrial or ventricular fibrillation. However, the current weight of evidence does not support the view that the irregular ventricular response in fibrillation itself represents deterministic cardiac chaos. An alternative hypothesis is that the subtle but complex heart rate fluctuations seen during normal sinus rhythm in individuals are attributable in part to deterministic chaos, and that various diseases may involve a paradoxical decrease in this type of non-linear variability[20]. The intriguing question of the role, if any, of chaos in physiology or pathology remains unresolved.

Examples of fractal like anatomies include the arterial and venous trees, the branching of certain cardiac muscle bundles, the tracheobronchial tree and His-Purkinje network. Mechanistically these self-similar structures

all serve a common physiological function: rapid and efficient transport over a complex spatially distributed system. Various other organ systems contain fractal structures that serve functions related to information distribution (the nervous system), nutrient absorption (bowel), and collection and transport (biliary duct system, renal calyces)[17].

Complex structures with the statistical properties of fractals have been described for heart rate variability, fluctuations in respiration[21], systemic blood pressure[22], human gait[23], white blood cell counts, and certain ion-channel kinetics[17].

If scale variance is a central organizing principle of physiological structure and function, we can make a general, but potentially useful prediction about what might happen when these systems are severely perturbed. If a functional system is self-organised in such a way that it does not have a characteristic scale of length or time, a reasonable anticipation would be a breakdown of scale free structure or dynamics with disease. The antithesis of a scale free system, i.e. one with many scales, is one that is dominated by one frequency or scale. A system that has only one dominant scale becomes easily to recognize and characterize, because such a system is by definition periodic, i.e. it repeats behavior in a highly predictable pattern[17].

The paradoxical appearance of periodic dynamics in many disease states in one of the most compelling examples of complexity loss in disease. Complexity refers specifically to multi-scale, fractal type of variability in structure of function. Many of the disease states are marked by less complex dynamics than those seen under healthy conditions[17]. This decomplexification of systems with disease seem a common feature of many diseases as well as aging[24]. Remarkably, the output of many severely pathological systems is nearly sinusoidal in appearance. For example, severe congestive heart failure and fetal distress syndrome[17].

Generally, the practice of bedside diagnosis would be impossible without the loss of complexity and the emergence of such pathological

periodicities[20]. It is these periodicities and highly structured patterns that allow clinicians to identify and classify many pathological features of their patients. Familiar examples include periodic tremors in neurological disease, AV Wenckebach patterns, the sine wave electrocardiogram pattern in hyperkalemia, manic depressive alternations and Cheyne-Stokes breathing patterns in heart failure[17].

Although fractals are irregular, not all irregular structures or erratic time series are fractal. An essential feature of the class of fractals seen in biology is a distinctive type of long range order[17] This property generates correlations that extend over many scales of space or time. Certain diseases are marked by a breakdown of this long-range organization property producing an uncorrelated randomness similar to white noise. An example is the erratic ventricular response in atrial fibrillation[17]

Practical applications of non-linear dynamics are likely to arise within the next few years. Probably the first bedside implementations will be in physiological monitoring[17] Several indices derived from chaos theory have shown promise in forecasting those at high risk of electrophysiological or hemodynamic instability, including heart rate alternans, ST-T alternans, breakdown in fractal scaling, differences or changes in the non-linear dimension or complexity of a time series[17]

Findings of non-linear dynamics have also challenged conventional mechanisms of physiological control based on classic homeostasis, which indicates that healthy systems seek to attain a constant steady state. By contrast non-linear systems with fractal dynamics behave as if they are driven far from equilibrium under bases conditions. This kind of complex variability, rather than a single homeostatic steady state, seems to define the free running function of many biological systems[17,20].

2.2.3 Recent advances in pharmacokinetics

Fractal washout curves for ^{15}O-labeled water in isolated, perfused rabbit hearts have recently been described[25]. These concepts are being incorporated into noncompartmental pharmacokinetic models, although the

question arises as to whether one can ascribe physical or physiological significance to time as a fractal, and whether the fractal so used can cast some light on the enigma of the power function[26].

2.2.4 Anaesthesiology

In 1990 Goodman[27] predicted that many anaesthesia applications would be forthcoming from the emerging science of non-linear dynamics. However, to date the literature does not bear this prediction out. The only publications to date have concerned heart rate variability[28].

2.3 Non linear models

A literature study was conducted to see if anyone had investigated the possibility that the absorption of inhalation agents was a non-linear process. Not a single reference could be found.

One article[29] investigating the uptake of oxygen during exercise identified a non-linear component above that which was expected for extrapolation of the linear relationship which lead the authors to conclude, " suggests that it [oxygen uptake] is not related to the pattern of motor unit recruitment in any simple way". However, this non-linear component was not further quantified.

2.4 References

[1] Severinghaus J.W. The Rate Of Uptake Of Nitrous Oxide In Man. Journal Of Clinical Investigation 1954:33;1183-1189.

[2] Lowe H.J.,Ernst E.A. The Quantitative Practice Of Anaesthesia - Use Of The Closed Circiut. Baltimore: Williams And Wilkins, 1981.

[3] Watt S.J., Cook L.B., Ohri S,Lockwood G.G. The Relationship Between Anaesthetic Uptake And Cardiac Output. Anaesthesia 1996:51;24-28.

[4] Bengston J.P.,Bengston A.,Stengvist O. Uptake Of Enflurane And Isoflurane During Spontaneous And Controlled Ventilation. Anaesthesia And Intensive Care 1992:20;191-195

[5] Hendrickx J.F.A.,Soetens M,Van Der Donck A,Meeuwins H,Smolders F, De Wolf A.M. Uptake Of Desflurane And Isoflurane During Closed Circuit Anaesthesia With Spontaneous And Controlled Mechanical Ventilation. Anaesthesia And Analgesia 1997:84;413-418

[6] Walker T.J., Chakrababarti M.K.,Lockwood G.G. Uptake Of Desflurane During Anaesthesia. Anaesthesia 1996:51;33-36

[7] Lockwood G.G.,Chakrabarti M.K., Whitwam J.G. The Uptake Of Isoflurane During Anaesthesia. Anaesthesia 1993:48;748-752.

[8] Couto Da Silva J.M., Mapleson W.W.,Vickers M.D. Quantitative Study Of Lowe's Square-Root-Of-Time Method Of Closed-System Aneasthesia. British Journal Of Anaesthesia 1997:79;103-112

[9] Westenskow D.R.,Jordaan W.S.,Hayes J.K., Uptake Of Enflurane: A Study Of The Variability Between Patients. British Journal Of Anaesthesia 1983:55;595-601.

[10] Zbinden A.M., Frei F.,Westenskow D.R., Thomson D.A., Control Of End-Tidal Halothane Concentration. Part B: Verification In Dogs. British Journal Of Anaesthesia 1986:58;563-71.

[11] Lin C.Y. Uptake Of Anaesthetic Gases And Vapours. Anaesthesia And Intensive Care 1994:22;363-373.

[12] O'Callaghan A.C.,Hawes D.W.,Ross J.A.S. Uptake Of Isoflurane During Clinical Anaesthesia. Servo-Control Of Liquid Anaesthetic Injection Into A Closed-Circuit Breathind System. British Journal Of Anaesthesia 1983:55;1061-4.

[13] Lerou J.G.C.,Dirksen R,Beneken Kolmer H.H.,Booij L.H.D.J. A System Model For Closed-Circuit Inhalation Anaesthesia. Anesthesiology 1991:75;345-355

[14] Vermeulen P.M.,Lerou J.G.C.,Dirksen R.,Booij L.H.D.,Borm G.F. A System Model For Halothane Closed-Circiut Anaesthesia. Anesthesiology 1995:83;515-527.

[15] Vermeulen P.M.,Lerou J.G.C.,Dirksen R.,Booij L.H.D.,Borm G.F. Repeated Enflurane Anaesthetics And Model Predictions: A Study Of The Variability In The Perdictive Performance Measures. British Journal Of Anaesthesia 1997:79;488-496.

[16] Meiss J.D. Frequently Asked Questions In Non-Linear Science. Version 1.1.2 Posted On Http://Amath.Colorado.Edu/Appm/Faculty/Jdm/Faq.Htm November 1996.

[17] Goldberger A.L. Non-Linear Dynamics For Clinicians: Chaos Theory, Fractals And Complexity At The Bedside. The Lancet 1996:347;1312-1314.

[18] Rigney D.R.,Goldberger A.L. Nonlinear Mechanics Of The Heart's Swinging During Pericardial Effusion. American Journal Of Physiology 1989:257;H1292-305.

[19] Rosembaum D.S.,Jackson L.E.,Smith J.M.,Garan H.,Ruskin J.N., Cohen R.J. Electrical Alternans And Vulnerability To Ventricular Arrhythmia. New England Journal Of Medicine 1994:330;235-241.

[20] Goldberger A.L., Rigney D.R.,West B.J. Chaos And Fractals In Human Physiology. Scientific American 1990:262;42-49.

[21] Szeto H.,Chen P.Y.,Decena J.A.,Cheng Y.,Wu D.L.,Dwyer G. Fractal Properties Of Fetal Breathing Dynamics. American Journal Of Physiology 1992:263;R141-47.

[22] Marsch D.J.,Osborn J.L.,Cowley A.W. Fluctuations In Arterial Pressure And Regulation Of Renal Blood Flow In Dogs. American Journal Of Physiology 1990:258;F1394-400.

[23] Hausdorff J.M.,Peng C-K.,Ladin Z.,Wei J.Y.,Goldberger A.L. Is Walking A Random Walk? Evidence For Long-Range Correlations In The Stride Interval Of Human Gait. Journal Of Applied Physiology 1995:78;349-58.

[24] Lipsitz L.A.,Goldberger A.L. Loss Of 'Complexity' And Aging:Potential Applications Of Fractals And Chaos Theory To Senesecence. Journal Of The American Medical Association. 1992:267;1806-1809.

[25] Bassingthwaighte J.B.,Beard D.A. Fractal ^{15}O-Water Washout From The Heart. Circulatory Research 1995:77;1212-1221.

[26] Norwhich K.H. Noncompartmental Models Of Whole-Body Clearance Of Tracers: A Review. Annals Of Biomedical Enginering 1997:25;421-439.

[27] Goodman N.W. Chaos In Anaethesia. Anaesthesia 1990:45;187-188.

[28] Fleisher L.A. Heart Rate Variability As An Assessment Of Cardiovascular Status. Journal Of Cardiothoracic And Vascular Anaesthesia 1996:10;569-671.

[29] Zoladz J.A., Rademaker A.C., Sargeant A.J. Non-Linear Relationship Between Oxygen Uptake And Power Output At High Intensities Of Exercise In Humans. Journal Of Physiology 1995:488;211-217.

3 Research Method

3.1 Aim

To investigate if the absorption of anaesthetic gases, using isoflurane and enflurane as examples, is a non-linear process.

3.2 Data required

A time series of gas absorption was used, consisting of the amount of gas absorbed and the time at which this took place.

This was not a comparative study but an experimental study to statistically prove that the absorption of isoflurane and enflurane is non-linear. With this deterministic analysis any individual's data can be decisively predictive. NB This is not possible with stochastic measurements.

3.3 Patient selection and anaesthetic technique

Patient data from twenty (20) patients undergoing general anaesthesia with controlled ventilation at the Pretoria Academic Hospital were used. Informed consent for the use of the data was obtained from the patients. (See attached consent form, Appendix A). The technique used was the decision of the anaesthesiologist administering anaesthesia, but only patients where the main anaesthetic used was isoflurane or enflurane were selected for the purposes of this study. Gas analysis data as displayed on the Datex monitor screen was recorded from 5 minutes after the induction of anaesthesia until about 50 minutes after the induction of anaesthesia. This yielded a time series with approximately 550 to 1000 readings per series. The number of points is sufficient for the analysis required[8].

3.4 Accuracy of Measurements

The anaesthetic agent concentration was measured by the Datex AS/3 or Datex Capnomac Ultima Anaesthesia monitors currently in use at the Pretoria Academic Hospital. Before each recording, the apparatus and recording device was calibrated. The accuracy of these measuring instruments is given by the manufacturer[1,2] as being accurate ≤ 0.2% for both the Datex AS/3 and the Datex Capnomac Ultima. This compares well to mass spectrometery which approaches accuracies of ≤ 0.01% if properly calibrated.[9]

3.5 Ethical considerations

No deviation from standard anaesthesia practice was required. No additional risk was incurred by the patient. Informed consent was required for the use of the patient data by the researcher. No personal information about the patient will be disclosed at any stage. The necessary approval of the Ethics Committee, Faculty of Medicine, University of Pretoria and Pretoria Academic Hospitals was obtained on 22/07/1998. An addendum to the original protocol was approved on 30/09/1998 allowing both enflurane and isoflurane to be used. The protocol was assigned protocol number 120/98.

3.6 Data processing

Data indicating gas absorption in a breath by breath fashion was recorded from the Datex monitors currently in use at the Pretoria Academic Hospital.

The inspiratory and expiratory isoflurane or enflurane concentrations was processed using Lin's[3] method to yield a time series of milliliters per breath of isoflurane or enflurane absorbed.

$$\text{Uptake of agent in ml} = CI\% \times \left[1 - \frac{Fa}{Fi}\right] \times \overset{*}{V}$$

CI: Inhalation agent concentration in inspired breath

$\dot{V}$: Tidal volume in milliliters

3.7 Hypothesis

The absorption of isoflurane and enflurane is a non-linear process. To detect nonlinearity four conditions must be met[4,5,12]:

3.7.1 Sensitivity to initial conditions

3.7.2 Fractal Dimension of the attractor

3.7.3 Invariant probability distribution of the attractor

3.7.4 Detection of an underlying dynamical process

3.8 Null hypothesis

The absorption of the anaesthetic agents Isoflurane and Enflurane is fully described by independent and identically distributed random variables[12], i.e. the variability seen in the absorption is random[6] and there is no underlying deterministic process.

The time series measured will be analytically indistinguishable from noise signals.

3.9 Data analysis

Numerous methods of analysis derived from classical signal processing or non-linear dynamics are available. No single measure is more appropriate than others for physiological research or clinical practice[7,8], on the contrary it is necessary to use a large panel of analysis techniques, rather than a single one, to investigate a time series[7]. This is in contrast with linear statistical practice where the greatest difficulty lies in selecting the appropriate test[9].

Therefore, a panel of tests recommended by Mansier et al[7] will be used in the analysis of the time series obtained. They are:

3.9.1 Time domain indexes

3.9.1.1 Mean

$$u = \frac{\sum Xi}{N}$$

u: Mean

Xi: Data points

N: Number of points in series

Reference [9]

3.9.1.2 Standard deviation

$$\sigma = \sqrt{\frac{\sum (Xi - u)^2}{N}}$$

σ: Standard deviation

u: Mean

Xi: Data points

N: Number of points in series

Reference [9]

3.9.2 Non-linear indexes

3.9.2.1 Sensitivity to initial conditions

Lyapunov exponents[7] allow the quantification of sensitive dependence on initial conditions. The first exponent λ_1, has to be positive for the system to be chaotic, but the following ones may be positive or negative. The sum $\Lambda=\lambda_1 + \lambda_2 + \ldots + \lambda_n$ gives the exponential rate Λ of the contraction (if positive) or expansion (if negative) of the system.

3.9.2.2 Fractal Dimension of the chaotic attractor

3.9.2.2.1 Embedding dimension or reconstructing the attractor

Using a method of delays, the one dimensional time series will be constructed into an *m* dimensional attractor[7]. The *m* dimension of the space in which one embeds the trajectory is called the embedding dimension. If this is large enough then the geometrical properties of the trajectory and of the reconstructed attractor are conserved by this processing. Statistical and geometrical variants of the attractor such as fractal dimension, Lyapunov exponents, and entropy can then be computed[7].

3.9.2.2.2 Measuring the attractor

3.9.2.2.2.1 Fractal dimension

Chaotic systems are drawn together towards attractors that have in most cases a non-integer dimension: i.e. fractal dimension[8]. This can be obtained by the box counting method[7].

3.9.2.2.2.2 Correlation dimension

Also a measure of the non-integer dimension of the attractor, which is computationally more efficient than the box counting method[8]. This can be obtained by the Grassberger-Proacaccia algoritm[7].

3.9.2.2.2.3 Information entropy

This is a quantification of the information uniformity carried by the probability distribution. In the case of a strange attractor where the measure considered is the counting measure on the trajectory, the information entropy is lower than the sum of positive Lyapunov exponents[7].

3.9.2.2.2.4 Approximate entropy

A variant of Information entropy has been proposed by Pincus et al[10], as less sensitive to noise and more suitable for short stationary time series, in the range from 500 to 1000 numbers[10].

3.9.2.3 Invariant probability distribution of attractor or unpredictability

Non linear forecasting described by Sugihara and May[11] is a method whereby apparent noise associated with deterministic chaos can be distinguished from sampling error and other sources of induced environmental noise.

3.9.2.4 Detection of an underlying dynamical process[12]

Comparison with surrogate data is a means of identifying non-linearity in a time series. Surrogate data is generated by one of three methods, namely Unwindowed Fourier transform, Windowed Fourier transform or Amplitude adjusted Fourier transform[12]. The surrogate data generated is then compared to the original. This developed "check" has been described as significant development in chaos research[8].

3.10 Computation

The above-mentioned analyses will be done using Microsoft Excel 8® (in licensed possession of the researcher), Santis, and DSN. (Two non-linear analyses programs, in public domain). Should it become necessary other software may also be used.

3.11 Power Analysis

A power analysis[13] using expected results[14] revealed that considering a p value (using a Student's T-test) of < 0.05 as significant, ten measured signals and ten noise signals in each group would be sufficient for a power >0.8.

3.12 Testing of the null hypotheses

3.12.1 Description

Each individual condition will be subject to testing. The isoflurane and enflurane groups will be individually compared to noise control signals.

A p value < 0.05 will be considered significant in each case. A power analysis will be done on each set of results and only accepted if the power > 0.8. If all four conditions are met for a gas, then the variability in the absorption will be considered non-linear, and the null hypothesis that the variability is random will be rejected.

3.12.2 Symbolic representation

3.12.2.1 Nul hypothesis

H_0: $\delta_G = \delta_N$

δ_G : Test statistic for measured time series

δ_N : Test statistic for noise signals

3.12.2.2 Hypothesis

H_{1A}: $\mu_G \neq \mu_N$ (Lyapunov exponents, H_{0A} : $\mu_G = \mu_N$)

H_{1B}: $\mu_G \neq \mu_N$ (Dimension, H_{0B} : $\mu_G = \mu_N$)

H_{1C}: $\pi > 0.5$ (Non-linear forecasting, H_{1C}: $\pi = 0.5$)

H_{1D} : $\mu_G \neq \mu_N$ (Surrogate data),

$H_{1D(I)}$: $\mu_G \neq \mu_{SD}$, $H_{0D(I)}$: $\mu_G = \mu_{SD}$, (Lyapunov exponent)

$H_{1D(II)}$: $\mu_G \neq \mu_{SD}$, $H_{0D(II)}$: $\mu_G = \mu_{SD}$, (Correlation Dimension)

The null hypothesis will be rejected for a gas, if H_{1A}, H_{1B}, H_{1C}, and H_{1D} are all found to be true.

The null hypothesis were rejected for a gas, if H_{1A}, H_{1B}, H_{1C}, and H_{1D} were all found to be true.

3.13 References

[1] Datex As/3 Anaesthesia Monitor Operator's Manual. Datex Division, Instrumentation Corporation, Helsinki, Finland. 1995:2-21.

[2] Datex Capnomac Ultima Anaesthesia Monitor Operator's Manual. Datex Division, Instrumentation Corporation, Helsinki, Finland. 1994:14-3

[3] Lin C.J. The Uptake Of Anaesthetic Agents. Anaesthesia And Intensive Care 1994:22:363

[4] Moon F.C. Chaotic And Fractal Dynamics: An Introduction For Applied Scientists And Engineers. John Wiley And Sons1992

[5] Bassingthwaighte J.B.,Liebovitch L.S.,Westb.J. Fractal Physiology. Oxford Universtity Press 1994.

[6] Cerutti S.,Carrault G.,Cluitmans P.J.M.,Kinie A.,Lipping T.,Nikolaidis N.,Pitas I., Signorini M.G. Non-Linear Algorithms For Processing Biological Signals. Computer Methods And Programs In Biomedicine 1996:51;51-73.

[7] Mansier P,Clairambault J,Charlotte N,Medigue C,Vermeiren C,Lepape G,Carre F,Gounaropoulou A,Swynghedauw B. Linear And Non-Linear Analyses Of Hear Rate Variability:A Mini Review. Cardiovascular Research 1996:31;371-379.

[8] Persson P.B.,Wagner C.D. General Principles Of Chaotic Dynamics. Cardiovascular Research 1996:31;332-341.

[9] Fisher D.M. Statistics In Anesthesia, Chapter 21 In Miller, R.D. Anesthesia 3rd Edition, Churchill Livingstone, 1990.

[10] Pincus S.M.,Goldberger A.L. Physiological Time-Series Analysis: What Does Regulatory Quantify?. American Journal Of Physiology 1994:266;H1643-H1656.

[11] Sugihara G.,May R.M. Nonlinear Forecasting As A Way Of Distinguishing Chaos From Measurement Error In Time Series. Nature 1990:344;734-741.

[12] Theiler J.,Eubank S.,Longtin A.,Gladrikian B.,Farmer J.D. Testing For Nonlinearity In Time Series: The Method Of Surrogate Data. Physica D 1992:58;77-94.

[13] Steyn A.G.W.,Smit C.F.,Du Toit S.H.C., Strasheim C. Modern Statistics In Practice. Jl Van Schaik 1996

[14] Wolf A.,Swift J.B.,Swinney H.L.,Vastano J.A. Determining Lyapunov Exponents From A Time Series. Physica D 1985:16;285-317.

4 Measured Time Series

4.1 Method

After measuring instrument calibration, the anaesthesia gas analysis displayed on the Datex Monitor screen was captured in a spreadsheet format using a personal computer (Siemens Nixdorf PCND). The anaesthetic agent to be used was up to the discretion of the anaesthesiologist administering the anaesthetic.

4.2 Characteristics

4.2.1 Description

A total of twenty times series were measured, each on a different patient. For ten, isoflurane was used as an anaesthetic and for ten, enflurane was used as an anaesthetic. The mean age of the patients was 50±20 (mean ± standard deviation) , with a range of 21 to 82 years. The mean mass of the patients was 61±14, with a range of 41 to 89 kilograms. Six of the ten patients in the isoflurane group were male, in comparison with five of the ten patients in the enflurane group. The mean number of points in the time series is 599±244 with a range of 254 to 1259 points.

4.2.2 Tabular Summary

FILE NAME	AGE	MASS (KG)	SEX	NUMBER OF POINTS	MEAN	STANDARD DEVIATION	TIDAL VOLUME
Iso-01	63	63	M	495	133.37	118.54	600
Iso-02	65	61	F	254	99.47	66.56	650
Iso-03	56	89	M	912	236.28	76.24	700
Iso-04	77	67	M	1259	175.75	98.59	650
Iso-05	34	78	M	854	147.68	49.79	550
Iso-06	23	50	F	641	140.72	69.53	500
Iso-07	24	45	F	276	127.36	104.09	300
Iso-08	65	43	F	341	183.35	72.06	250
Iso-09	68	41	M	753	54.42	20.38	375
Iso-10	45	70	M	664	113.55`	58.11	450

Table 4-1 Tabular Summary Of The Measured Time Series For Isoflurane

FILE NAME	AGE	MASS (KG)	SEX	NUMBER OF POINTS	MEAN	STANDARD DEVIATION	TIDAL VOLUME
Enf-01	77	65	F	387	366.49	63.73	500
Enf-02	34	63	F	472	170.2	82.63	385
Enf-03	21	60	M	383	253.02	104.21	385
Enf-04	82	62	M	636	162.45	71.71	400
Enf-05	34	44	M	692	49.55	2.688	300
Enf-06	34	55	M	377	196.54	248.81	350
Enf-07	30	58	F	637	224.7	133.47	450
Enf-08	72	85	M	504	160.71	61.11	600
Enf-09	65	83	F	708	99.27	5.46	550
Enf-10	43	55	F	740	160.69	63.17	450

Table 4-2 Tabular Summary Of The Measured Time Series For Enflurane

A full listing of the measured time series is to be found in Appendix B.

5 Dimension

5.1 Definition

The description "strange attractor" has been used to describe nonperiodic, randomlike time series, describing the unfamiliar geometric structure on which the series moves in phase space[1]. The quantitative measure of the "strangeness" of the attractor is described by its dimension[1], dimension being the first level of knowledge necessary to characterize its properties. Dimension may be thought of as giving the amount of information necessary to specify the position of a point on the attractor within a given accuracy[2].

5.2 Discussion

The revolution in nonlinear dynamics has been sparked by the introduction of new geometric, analytic, and topological ideas, which have given experimentalists and numerical analysts new tools to analyze dynamical processes. This in some ways parallels the earlier Newtonian revolution, which introduced the calculus into dynamics. Thus in some ways we are entering the second phase of the Newtonian revolution in dynamics[1].

5.2.1 Classical Fractals and Self-Similarity

Mandelbrot is often called the father of fractal geometry, although fractals and their description go back to classical mathematics and mathematicians of the past like Cantor (1872), Peano (1890), Hilbert (1891), von Kock (1904), Sierpinski (1916), Julia (1918) and Huasdorff (1919) to name a few examples[3]. The creations of these mathematicians played an essential role in Mandelbrot's concept of new geometry, although they did not think of their creations as conceptual steps towards a new perception or a new geometry of nature. On the contrary, their creations, for example the Cantor Set and the Koch curves, were regarded as exceptional objects, as counter examples, as "Mathematical Monsters"[3]. These were seen as

shapes, intended to demonstrate the deviation from the familiar rather than typify the normal.

Mandelbrot was the first to demonstrate that these early mathematical fractals in fact had many features in common with shapes found in nature. He turned the manifested mathematical interpretation and value of these inventions upside down, and furthermore went on to develop a language into which these characters could be embedded. Noticing that the seemingly exceptional is more like the rule and then developing a systematic language with words, sentences, and grammar[3], Mandelbrot called this a summary of scientific experiments in mathematics, linguistics, economics, physics, medical sciences and communication networks to mention just a few areas in which he was involved[3].

5.2.2 Fractals and the problem of dimension

The original concepts of dimension originated in topology, a branch of mathematics that deals with form and shape from a qualitative point of view. Two of its basic notions are "dimension" and "homeomorphism." Straight lines can be bent into curves and circles can be pinched into triangles or pulled into squares, but not everything is topologically interchangeable[3]. The intersection of two lines, for example, remain an intersection, the number of holes in an object is also a topological invariant. The transformations, which are applied, are called homeomorphisms, and when applied they must not change the invariant properties of the objects[3]. Thus, a sphere and a cube are homeomorphic, but the sphere and a doughnut are not. In the development of topology, mathematicians looked for qualitative features, which would not change when the objects were transformed properly, technically by a homeomorphism, but preserving the dimension[3]. But it turned out there were severe difficulties in arriving at a proper and detailed notion of dimension that would behave in that way[3].

During this century, mathematicians came up with many different notions of dimension such as small inductive dimension, large inductive dimension, covering dimension, and homological dimension[4]. Some of

these are topological in nature; their value is always a number or zero for points and does not change for topologically equivalent objects[3].

In attempting to measure complex objects, the questions of length, area and volume can be ill posed. Curves, surfaces, and volumes can become so complex that these ordinary measurements become meaningless. However, it is possible to measure the degree of complexity by evaluating how fast length, or surface, or volume increases if one measures with respect to smaller and smaller scales. The fundamental idea is to assume the two qualities, length, or surface or volume on the one hand, and scale on the other hand are not arbitrarily but rather are related by a law[3]. This law will allow one to compute one quantity from the other. The law that seems to be relevant is the power law in the form of $y \propto x^d$.

The power law can be summarizes as follows:[3] if the x and y data of an experiment range over very large numerical scales, then it is possible that there is a power law which expresses y in terms of x, $y \alpha x^d$. To test the power law conjecture a plot of the data is made in a log/log plot. If then, the measurements fit a straight line, the exponent can be read off as the slope of the line.

Such a law turns out to be very useful for the discussion of dimension. The problem of dimension has not been made easier to understand with the description of at least ten different kinds of dimension since the turn of the century[3]. They are all related. Some of them make sense in certain situations, but not in others, sometimes they make sense and are the same, sometimes several make sense, but do not agree. The details can be confusing even to the research mathematician[3].

For the purposes of this thesis, dealing with a biological time series, the discussion of dimension will be limited to those dimensions, which have been found useful for analyzing biological time series. They are fractal dimension, information dimension and correlation dimension[5,6] .

The issue is further confused by the lack of uniformity of definitions. For example Farmer et al[2] consider the capacity and the Hausdorff

dimensions as metric dimensions and groups them under the heading "Fractal Dimension", and information dimension and pointwise dimension as dimensions of the "Natural Measure". This is in contrast with Moon[1], who classifies the pointwise dimension and the information dimension as measures of the fractal dimension! For the purpose of this thesis, the definitions used will be taken from Mansier et al[5], being the most recent reference to discuss all three dimensions that are to be calculated.

5.2.3 Fractal dimension

This dimension is calculated using the box counting method[5] and is sometimes called the "Box Counting Dimension"[3]. The box counting method proposes a systematic measurement of any structure in the plane under consideration and can be readily adapted for structures in space.

The structure under consideration is placed on a regular mesh with mesh size s, and the number of grid boxes which contain some of the structure are counted[3]. This gives a number, N; the value of which depends on the choice of s and so is denoted as $N(s)$. S is changed to progressively smaller sizes and the corresponding number $N(s)$ is counted. A log/log diagram is then plotted of $\log(N(s)) / \log(1/s)$. A straight line is then plotted to the points of the diagram and its slope D_b is measured. This number is the fractal dimension[3].

This dimension is one of the most commonly used dimensions. The reason for its dominance lies in easy and automatic calculation by computer. It is straight forward to count boxes and to maintain statistics allowing dimension counting. The program can be used for shapes with and without self-similarity. Moreover, the objects can be embedded in higher dimensional spaces[3].

A formal definition of the box counting dimension is given by Peitgen et al[3]:

The box counting dimension is D_B of any bounded subset A of R^n.

Let $N_\delta(A)$ be the smallest number of sets of diameter at most, δ which cover A. Then:

$$D_b(A) = \lim_{\delta \to 0} \frac{\log N_\delta(A)}{\log 1/\delta}$$

provided that the limit exists.

Roughly speaking the definition says that $N_\delta(A) \ \alpha \ \delta^s$ for small δ, where $s=D_{(b)}(A)$.

More precisely, it says that:

$$N_\delta(A)\delta^s \rightarrow \left\{ \frac{\infty \ for \ s < D_b(A)}{0 \ for \ s > D_b(A)} \right\}$$

5.2.4 Information dimension

The information dimension gives an idea of the natural measure of an attractor[2,3]. In computing the box counting dimension the cubes used in covering the attractor are equally important although the frequencies with which an orbit on the attractor visits these cubes may be very different. In order to take the frequency, with which each cube is visited into account, the relative frequency with which a typical orbit visits different regions of the attractor must also be taken into account[2]. The natural measure gives the relative probability of different regions of the attractor as obtained from the averages, and is therefore "natural" to consider[2].

The information dimension is a generalization of the capacity that takes into account the relative probability of the cubes used to cover the set. This dimension was originally introduced by Balatoni and Renyi[2].

The information dimension is given by

$$d_i = \lim_{\varepsilon \to 0} \frac{I(\varepsilon)}{\log(1/\varepsilon)}$$

Where

$$I(\varepsilon)=\sum_{i=1}^{N(\varepsilon)} P_i \log\frac{1}{p_i}$$

and P_I is the probability contained in the I^{th} cube. Letting the i^{th} cube of side ε be C_I, $P_I=\mu(C_I)$. Note that if all cubes have equal probability then $I_{(\varepsilon)}=logN_{(\varepsilon)}$, and hence $d_c=d_I$. However for unequal probabilities $I_{(\varepsilon)}<logN_{9\varepsilon)}$. Thus in general $d_c>d_I$, where d_c is the box counting dimension.

$I_{(\varepsilon)}$ is the amount of information necessary to specify the state of the system to within an accuracy of ε. The information dimension may therefore be viewed as telling how fast the information necessary to specify a point on the attractor increases as ε decreases[2]. Stated otherwise it may be viewed as a measure of the unpredictability in a system[1].

5.2.5 Correlation dimension

This dimension is the exponent of the power law dependence of the correlation integral as a measure of the strangeness of an attractor[7]. It has been successfully used by many experimentalists and is in some ways related to the pointwise dimension[1].

To calculate the correlation dimension the orbits of an attractor are discretized in phase space. One then calculates the distances between the pairs of points using either conventional Euclidean measure of distance (square root of the sum of the squares of the components) or some equivalent measure such as the sum of absolute values of vector components. A correlation function is then defined as[1]:

$$C(r)=\lim_{N\to\infty}\frac{1}{N^2}\left(\frac{number\ of\ pairs\ (i,j)}{with\ dist-ance\ s_{ij}<r}\right)$$

For many attractors this function has been found to exhibit a power law dependence on r as $r\to 0$; that is,

$$\lim_{r\to 0} C(r)=ar^d$$

So that one may define a correlation dimension using the slope of the ln C versus ln r curve:

$$d_G = \lim_{r \to 0} \frac{\log C(r)}{\log r}$$

It has been shown that $C(r)$ may be calculated more effectively by constructing a sphere or cube at each point x_i in phase space and counting the number of points in each sphere. That is:

$$C(r) = \lim_{r \to 0} \frac{1}{N^2} \sum_{i}^{N} \sum_{j}^{N} H(r - |x_i - x_j|)$$

Where $H(s)=1$ if $s>0$ and $H(s)=0$if $s<0$. This differs form the pointwise dimension in that the sum here is performed about every point[1].

5.3 Computational algorithms

The program SANTIS has the facility to calculate the Correlation Dimension using the Grassberger Procaccia algorithm[8]. Neither of the two programs used had the facility to calculate either the Fractal dimension or the Information dimension. A programmatic solution was developed using Microsoft Excel version 8® and Microsoft Visual Basic for Applications®.

The code for the programmatic solution for the fractal dimension can be found in Appendix F and the code for the programmatic solution for the information dimension can be found in Appendix G.

5.3.1 Computational description

The fractal dimension is calculated by putting the structure onto a regular mesh with a mesh size s and counting the number of grid boxes, which contain some of the structure. The mesh sizes are made progressively smaller and the process repeated. A log/log-diagram is then constructed and a straight line fitted to the plotted points of the diagram. The slope of this line is now measured and this is the fractal dimension[3]. For the information

dimension the number of grid boxes containing structure are weighted according to the number of orbits contained in a specific box, using the probability of finding a point in that cell[1].

5.3.2 Computational solution

The time series to be analyzed is put into an array structure, the maximum and minimum values are determined. The user is asked then to enter the maximum number of boxes required in the mesh structure. Box sizes are then calculated from 1 box to the maximum number specified, with the grid size being calculated from the values in the time series and the number of boxes required by the user. To calculate the information dimension, the number of points in a box are added up and weighted according to the formula in 5.2.4. to calculate the fractal dimension the number of boxes containing structure are summed.

These stored values are then entered into a log/log-plot, and the slope of the regression line is determined, which is the dimension that is desired, either fractal or infomation.

5.4 Programmatic solution

The program for both the fractal dimension and for the information dimension was developed using Microsoft Excel version 8®, using Visual Basic for Applications. The time series under consideration is pasted into a range and then a runtime resizable array. The time series maximum and minimum values are used to calculate the box sizes up to the maximum number of boxes specified. The counting procedure is done in a loop. The values calculated are stored in an array. These values are later pasted into a new range from which a graph is constructed. Microsoft graph® does not have the facility to construct log/log graphs. To overcome this problem, the required log conversions of the numbers are done first in the spreadsheet and then a graph is constructed from the converted values. Using linear regression, the slope of the graph is then calculated.

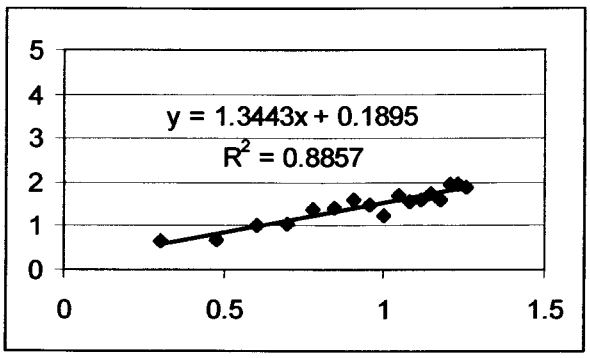

Figure 5-1 Example of log/log plot and regression line with slope created by the information dimension program.

5.4.1 Testing the programs

5.4.1.1 Method

The programs written and the SANTIS correlation dimension feature were tested, to see if they could measure the information, fractal, and correlation dimensions accurately. The null hypothesis is that they are unable to distinguish known chaos from noise. A Henon time series and Logistic map with a starting value 0.2 and a delta value of 3.8 were used as known chaotic series[1] (These two time series may be found in Appendix E). Four noise series generated by SANTIS were used as control series (These four time series may be found in Appendix D). A Student's T-test was used as the test statistic and a p value of <0.05 was considered significant, in order to reject the null hypothesis.

5.4.1.2 Results

	HENON	LOGISTIC MAP	NOISE1	NOISE2	NOISE3	NOISE4	P
Information Dimension	1.370	2.140	0.854	0.850	1.120	0.944	0.0164
Correlation Dimension	1.245	0.933	3.039	3.039	3.039	2.986	0.000038
Fractal Dimension	0.990	1.025	0.948	0.940	0.940	0.850	0.0366

Table 5-1 Calculated dimensions for known chaos and known noise signals

The p values calculated were 0.0164, 0.000038, and 0.0366 for the information dimension, correlation dimension, and the fractal dimension respectively. They are all less than 0.05 and therefore the null hypothesis is rejected and it is concluded that the programs are successfully able to differentiate known chaos from known noise.

5.5 The dimensions of the recorded times series

The dimensions were calculated in the same manner for the twenty measured time series. The time series are to be found in Appendix B.

FILE NAME	INFORMATION DIMENSION	CORRELATION DIMENSION	FRACTAL DIMENSION
Iso-01	1.504	0.785141	0.864
Iso-02	1.52	1.48417	1.068
Iso-03	1.41	0.952904	0.847
Iso-04	1.586	1.03614	1.13
Iso-05	1.64	1.50338	0.989
Iso-06	1.338	1.3673	1.17
Iso-07	0.917	1.04189	0.987
Iso-08	1.38	1.36093	1.15
Iso-09	0	1.52047	0
Iso-10	0	1.57578	0.8521
Enf-01	0.0634	1.88901	0.476
Enf-02	1.9	0.814319	0.9622
Enf-03	1.949	0.975127	1.04
Enf-04	1.84	1.81347	0.894
Enf-05	0	0.0982057	0
Enf-06	1.24	1.46198	0.94
Enf-07	1.47	1.46198	1.035
Enf-08	1.67	1.23643	0.862
Enf-09	0	0.101749	0
Enf-10	1.57	0.80455	0.672

Table 5-2 Dimensions of the measured time series

5.6 The dimensions of the control noise times series

NOISE SIGNAL	INFORMATION DIMENSION	CORRELATION DIMENSION	FRACTAL DIMENSION
1	1.352	2.98029	1
2	1.972	2.92491	0.965
3	1.9707	2.94902	1.018
4	2.0346	2.93406	0.984
5	1.6275	2.95673	0.910
6	1.9972	3.33461	1.0354
7	1.8233	2.9325	1.0554
8	1.884	3.12329	0.9182
9	1.8115	2.93593	1.0885
10	2.0456	2.80135	0.9991

Table 5-3 Dimensions of the control noise time series

5.7 Statistical Analysis

The hypothesis and null hypothesis were formulated and stated in chapter 3, and are repeated here for clarity sake.

5.7.1 Hypothesis

The absorption of isoflurane and enflurane is a non-linear process. To detect nonlinearity four conditions must be met:

- Fractal Dimension of the attractor
- Sensitivity to initial conditions

- Invariant probability distribution of the attractor
- Detection of an underlying dynamical process

5.7.1.1 Null hypothesis

The absorption of the anaesthetic agents Isoflurane and Enflurane is fully described by independent and identically distributed random variables, i.e. the variability seen in the absorption is random[9] and there is no underlying deterministic process.

The time series measured will be analytically indistinguishable from noise signals.

5.7.1.2 Fractal Dimension of the attractor

This part of the hypothesis is being tested by this chapter.

5.7.2 Statistical Methods and Tests

The information dimension, the fractal dimension and the correlation dimension for each of the measured time series was compared to the information dimension, fractal dimension and correlation dimensions of a control noise series. The isoflurane and enflurane measured time series were treated as separate groups and each was individually compared to the noise series control group.

A Student's T-test was used to compare the measured and the control groups, with, as stipulated in chapter 3 a p value of < 0.05 being considered significant.

5.7.3 Results

	INFORMATION DIMENSION	CORRELATION DIMENSION	FRACTAL DIMENSION
Isoflurane group	0.005435	<0.00000	0.2133
Enflurnane group.	0.028838	0.000003	0.038049

Table 5-4 Results of the Student's T-test comparisons for the two groups of measured time series

All the Student's T-test comparisons yield p values of <0.05 except for the fractal dimension of the isoflurane measured series and the noise group. These results strongly recommend the acceptance of the hypothesis stated above (5.7.1) and more specifically, that there is evidence for a fractal attractor underlying the measured time series for both isoflurane and enflurane.

5.7.3.1 Isoflurane Fractal Dimension

The fractal dimension or box counting dimension[3] as termed in some literature is the eldest of the measures of dimension, being based on work done by Hausdorff in 1919. As the number of computations are increased the log/log plot is no longer a straight line and therefore it becomes impossible to accurately measure the fractal dimension and the results reported often underestimate the dimension[3]. These shortcomings have lead investigators to sometimes give up using the fractal dimension or look for alternatives such as the information dimension[1] etc.

Bearing these facts in mind, it is concluded that not too much significance should be drawn from the fact that the t test was unable to distinguish the isoflurane measured time series from the noise series.

5.7.4 Power Analysis

To prevent a type II statistical error from being made, where the null hypothesis is accepted when the hypothesis is actually true, a power analysis[10] was performed. For the analysis, an alpha level of 2.35 was used which corresponds to a p value of <0.01 for the rejection of the null hypothesis. A power level of >0.8 was considered acceptable[10].

5.7.4.1 Power analysis for Isoflurane group

5.7.4.1.1 Information Dimension

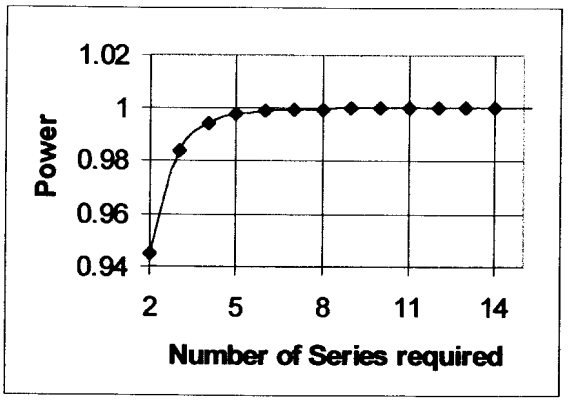

Figure 5-2 Power of the Student's T-test for the isoflurane measured time series

5.7.4.1.2 Fractal Dimension

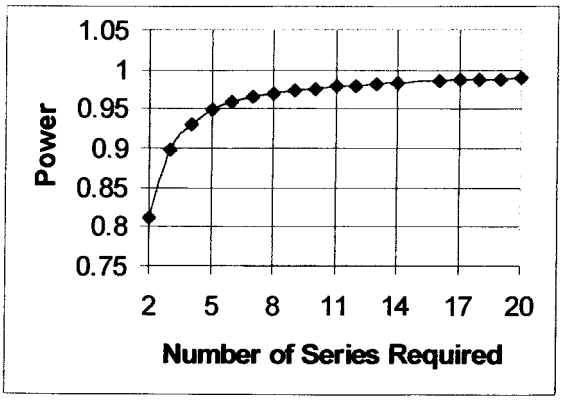

Figure 5-3 Power of Student's T-test for isoflurane measured time series

5.7.4.1.3 Correlation Dimension

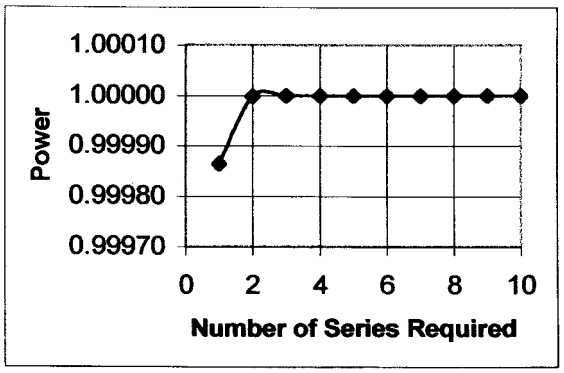

Figure 5-4 Power of Student's T-test for isoflurane measured time series

5.7.4.2 Power analysis for Enflurane group

5.7.4.2.1 Information Dimension

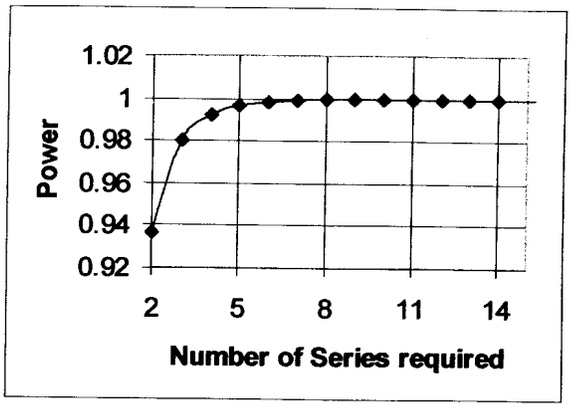

Figure 5-5 Power of Student's T-test for enflurane measured time series

5.7.4.2.2 Fractal Dimension

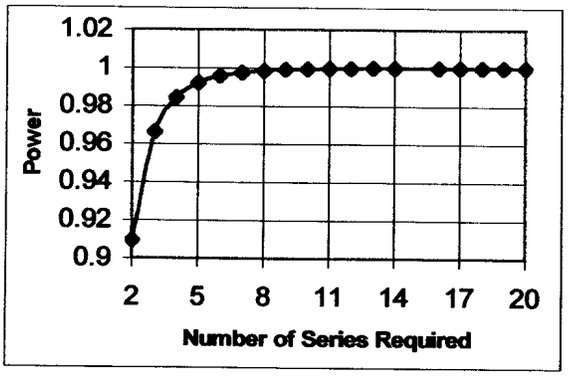

Figure 5-6 Power of the Student's T-test for the enflurane measured time series

5.7.4.2.3 Correlation Dimension

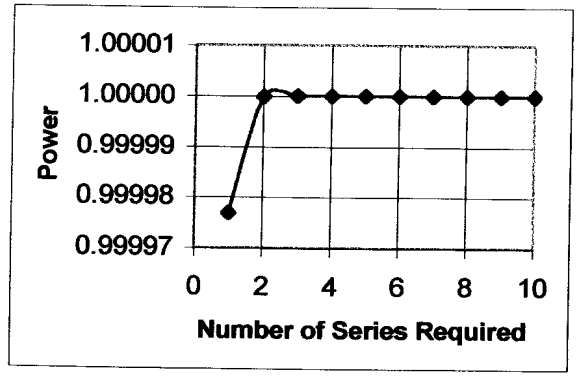

Figure 5-7 Power of Student's T-test for enflurane measured time series

5.7.4.3 Power Analysis Conclusion

Twenty series were used in each of the Student's T-test analyses. All the power analysis showed that this was more than adequate for a power of > 0.8 and a p value of < 0.01.

5.7.5 Conclusion

The results presented above show that there is evidence for a fractal attractor underlying the absorption of both isoflurane and enflurane. These results reach statistical significance ($p<0.05$) with acceptable statistical power (>0.8).

5.8 References

[1] Moon F.C. Chaotic And Fractal Dynamics: An Introduction For Applied Scientists And Engineers. John Wiley And Sons1992.

[2] Farmer J.D.,Ott F.,Yourke J.A. The Dimension Of Chaotic Attractors. Physicad 1983:7;153-180.

[3] Pietgen H.,Jurgens H.,Saupe D. Chaos And Fractals New Frontiers Of Science. Springer-Verlag 1992.

[4] Engelking R. Dimension Theory. North Holland 1978.

[5] Mansier P.,Clairambault J.,Charlotte N.,Medigue C.,Vermeiren C.,Lepape G.,Carre F.,Gounaropoulou A.,Swynghedauw B. Linear And Non-Linear Analyses Of Heart Rate Variability: A Minireview. Cardiovascular Research 1996:31;371-379.

[6] Cerutti S.,Carrault G.,Cluitmans P.J.M.,Kinie K.,Lipping T.,Nikolaidis N., Pitas I.,Signorini M.G. Non-Linear Algorithms For Processing Biological Signals. Computer Methods And Programs In Biomedicine 1996:51;51-73.

[7] Grassberger P.,Procaccia I. Characterization Of Strange Attractors. Physical Review Letters 1983:50;346-349.

[8] Vandenhouten R.,Rasche M.,Tegtmeier H.,Goebbels G. SANTIS User Manual. Institute Of Physiology, University Of Aachen 1996.

[9] Cerutti S.,Carrault G.,Cluitmans P.J.M.,Kinie A.,Lipping T.,Nikolaidis N.,Pitas I., Signorini M.G. Non-Linear Algorithms For Processing Biological Signals. Computer Methods And Programs In Biomedicine 1996:51;51-73.

[10] Steyn A.G.W.,Smit C.F.,Du Toit S.H.C., Strasheim C. Modern Statistics In Practice. JL Van Schaik 1996

6 Approximate Entropy

6.1 Definition

Approximate Entropy is the natural information theoretical parameter for an approximating Markov Chain to a process[1]. It is a recently developed statistic quantifying regulatory and complexity that appears to have potential application to a wide variety of physiological and clinical time-series data, including quantifying chaotic systems.

6.2 Discussion

In applications to a range of medical settings, findings have associated sickness and aging with significantly decreased Approximate Entropy values, consistent with the general hypothesis associating compromised physiology in many systems with more regular, patterned sinus rhythm heart rate tracings, and normative physiology in many systems with greater irregularity[1]. Findings implicitly associating greater regularity with compromised physiological status have been found elsewhere, including spectral analysis of heart rate in preterm babies[2], sudden infant death syndrome babies[3], in adult sudden death syndrome victims and in analysis of electrocardiographic waveforms during fatal ventricular tachyarrythmias[4]. These findings have produced qualitatively interesting results but lack a clear-cut statistic that summarizes the frequency spectra or underlying system structure[1].

In order to calculate Approximate Entropy two input parameters m and r must be fixed. M is the "length" of the compared runs and r is effectively a filter. Clinically, relatively low Approximate Entropy values (e.g., for heart rate) appear to correlate with pathology[1]. Greater non-linearity causes larger Approximate Entropy values. Greater stochastic influence produces larger Approximate Entropy values. Both greater ensemble non-linear and stochastic effects are manifested visually in greater randomness and complexity.

Approximate Entropy is a regularity parameter, and discerning changes in apparently random to very regular is the primary focus of this parameter[1].

The historical development of mathematics to quantify regularity has centered on various types of entropy measures. Entropy addresses system randomness and predictability. Greater entropy is associated with more randomness and less system order[1].

There are numerous entropy formulations and many entropy definitions, which often cannot relate to one another. K-S entropy, developed by Kolmogorov allows one to classify deterministic systems by rates of information generation[1]. This form of entropy can be estimated by algorithms such as the Grassberger and Procaccia[5] algorithm or the Eckmann and Ruelle[6] algorithm. There has been keen interest shown in these algorithms in the last 10 years[1], since entropy has been shown a parameter that characterizes chaotic behavior[7].

K-S entropy was not developed for statistical application. It is primarily applied by ergodic theorists to well defined theoretical transformations, with no noise, and an almost infinite amount of data[1]. It is compromised by steady, small amounts of noise, and generally requires a vast amount of input data to achieve a convergence[8], 10 000 points or more.

Approximate Entropy was constructed along thematically similar lines to K-S entropy, though with a different focus[1]. This was to promote a widely applicable statistically valid formula for the data analyst that will distinguish data sets by a measure of regularity. The intuition motivating Approximate Entropy is that, if joint probability measures for reconstructed dynamics that describe each of the two systems are different, then their marginal probability distributions on a fixed partition are probably different.

Orders of magnitude of fewer points are needed to accurately estimate these marginal probabilities than to accurately reconstruct the "attractor" measure defining the process[1].

Approximate Entropy has three technical advantages over K-S entropy. Approximate Entropy is nearly unaffected by noise of magnitude below r, the filter level. It is robust to occasional, very large or small artifacts, it gives meaningful information with a reasonable number of data points, and is finite for both stochastically and deterministic processes[1].

6.3 Computation Algorithms

6.3.1 Computational description

Two input parameters m and r are fixed. M is the "length" of compared runs, and r is effectively a filter. For a fixed m and r, the parameter Approximate Entropy (m,r) and the statistical estimate Approximate Entropy(N,m,r), given N data points $\mu(1)$, $\mu(2)$... $\mu(N)$ are defined.

Given N data points $\{\mu(i)\}$, form vector sequences $x(i)$ through $x(N-m+1)$, defined by $x(I)=[\ \mu(i),...\ \mu(N+m-1)]$. These vectors represent m consecutive μ values, commencing with the i^{th} point.

Define the distance $d[x(i),x(j)]$ between vectors, with $x(i)$ and $x(j)$ as the maximum difference in their respective scalar components. Use the sequence $x(1),x(2)....\ x(N-m+1)$ to construct for each $i \leq N-m+1$, $C_I^m(r)=$*(number of* $j \leq N+m-1$*)* such that $d[x(i),\ x(j)] \leq r / (N-m+1)$. The $C_I^m(r)$ values measure within a tolerance r the regularity or frequency of patterns similar to a given pattern of window length m. Define $\phi m(r) = (N-m+1)-1\ \sum N-1+mI=1\ ln(CIm(r))$, where ln is the natural logarithm, and then define the parameter Approximate Entropy$(m,r) = lim_{N\to\infty}[\phi m(r)-\phi m+1(r)]^1$.

Approximate Entropy is a measure of the logarithmic likelihood that runs of patterns that are close for m observations remain close on next incremental comparisons. The greater the likelihood of remaining close, produces smaller Approximate Entropy values and vice versa[1].

6.3.2 Computational solution

This is described as a number of steps[1]:

6.3.2.1 Step one

Focus on a specific length 2 vector, called for example *x(44)*. The conditional probabilities will be calculated for all length 2 vectors, then log averaged.

6.3.2.2 Step two

Identify all the length 2 vectors that are component wise close to vector *x(44)*, using the *r*-value to define "close."

6.3.2.3 Step three

Compute the conditional probability that the identified vectors are close to the original vector plus two, *x(46)*. The probability ratio A/B is calculated where A is the number of instances where the length 2 vector is close to *x(46)* and B the number of instances that the length 2 vector is close to *x(44)*.

6.3.2.4 Step four

Repeat steps one to three for each length 2-vector *x(i)*, calculating the conditional probability in each case. Calculate the average of the logarithm of these probabilities. The negative of this value is the Approximate Entropy. The negative of the log is used to ensure a positive result.

The opposing extremes are a perfectly regular sequence, e.g. sinusoidal behavior, which produces very low Approximate Entropy and independent sequential processes, e.g. random walk, which produces very large Approximate Entropy.

6.3.3 Implementation and interpretation

The value of N for Approximate Entropy is typically between 100 (one hundred) and 5000 (five thousand). Based on theoretical analysis and clinical application it has been concluded that for $m=2$ and $N=1000$, values of r from 0.1 to 0.25 of the standard deviation of the $\mu(i)$ data produce good statistical validity for Approximate Entropy(N,m,r) for many models[1].

Theoretical calculations indicate reasonable estimates of these probabilities are achieved with a N value of at least 10^m and preferably at least 30^m points[1], analogous to results for correlation dimension[8]. For r values smaller than 0.1 of the standard deviation one usually achieves poor conditional probability estimates as well, whereas r values larger than 0.25 the standard deviation, too much detailed system information is lost[1].

6.4 Programmatic solution

Neither of the two non-linear programs, SANTIS and DSN offered calculation facilities for Approximate Entropy. A programmatic solution was developed using Microsoft Excel version 8® and Microsoft Visual Basic for Applications®.

The code for the programmatic solution is found in Appendix H.

6.4.1 Programmatic considerations

The program was developed using the algorithm as described in section 6.3. A Macro was written for Microsoft Excel Version 8 using Microsoft Visual Basic for Applications. The user first places the time series to be analyzed in column A of Sheet 1 of the Approximate Entropy Workbook. The user is then asked to enter the number of points in the time series to be analyzed. The mean and standard deviation of the time series are then calculated. The user is then asked for the r (filter) value that is to be used. A value of 0.24 times the Standard deviation of the time series was used throughout the analyses for this thesis. This is within the recommendations made by Pincus et al [1]. An embedding dimension of is

then selected for the analysis. A value of two (2) was used throughout the analyses for this thesis, being appropriate for the size of the time series under consideration[1].

Using a series of nested loops[9] the time series is analyzed as described in section 1.3 for each two-length vector in the time series. For a time series consisting of one thousand points, this involves over one million runs through the loop, with 5 decisions and at least one calculation per loop! Each calculated probability is stored in a variable and the negative log of the average is then the approximate entropy of the time series.

6.4.2 Testing the Program

6.4.2.1 Method

The program written was tested to see if it could measure the approximate entropy accurately. The null hypothesis is that it is unable to distinguish known chaos from noise. A Henon time series and Logistic map with a starting value 0.2 and a delta value of 3.8 were used as known chaotic series[7] (These two time series may be found in Appendix E). Four noise series generated by SANTIS were used as control series (These four time series may be found in Appendix D). A Student's T-test was used as the test statistic and a p value of <0.05 was considered significant, in order to reject the null hypothesis.

6.4.2.2 Results

SIGNAL	HENON	LOGISTIC MAP	NOISE1	NOISE2	NOISE3	NOISE 4	P
Approximate Entropy	0.278	0.195	0.119	0.090	0.119	0.108	0.0096

Table 6-1 Calculated approximate entropy for known chaos And Known Noise

The calculated p value was 0.0096. This is less than 0.05 and therefore the null hypothesis is rejected and it is concluded that the program is successfully able to differentiate known chaos from known noise.

6.5 *Approximate Entropy of the measured time series*

The Approximate Entropy was calculated in the same manner for the twenty measured time series. The time series are to be found in Appendix B.

TIME SERIES	APPROXIMATE ENTROPY
Iso-01	0.066
Iso-02	0.113
Iso-03	0.144
Iso-04	0.095
Iso-05	0.121
Iso-06	0.133
Iso-07	0.062
Iso-08	0.03
Iso-09	0.243
Iso-10	0.127
Enf-01	0.204
Enf-02	0.132
Enf-03	0.087
Enf-04	0.183
Enf-05	0
Enf-06	0.056
Enf-07	0.143
Enf-08	0.125
Enf-09	0
Enf-10	0.13

Table 6-2 Approximate entropy values for the measured time series

6.6 Approximate Entropy of the control Noise time Series

NOISE SIGNAL	APPROXIMATE ENTROPY
1	0.01101
2	0.01105
3	0.00708
4	0.09901
5	0.0689
6	0.02084
7	0.013347
8	0.023086
9	0.000701
10	0.008503

Table 6-3 Approximate entropy of the control noise signals

6.7 Statistical Analysis

The hypothesis and null hypothesis were formulated and stated in chapter 3, and are repeated here for clarity sake.

6.7.1 Hypothesis

The absorption of isoflurane and enflurane is a non-linear process. To detect nonlinearity four conditions must be met:

- Fractal Dimension of the attractor
- Sensitivity to initial conditions
- Invariant probability distribution of the attractor
- Detection of an underlying dynamical process

6.7.1.1 Null hypothesis

The absorption of the anaesthetic agents Isoflurane and Enflurane is fully described by independent and identically distributed random variables, i.e. the variability seen in the absorption is random[10] and there is no underlying deterministic process.

The time series measured will be analytically indistinguishable from noise signals.

6.7.1.2 Fractal Dimension of the attractor

This chapter is testing this part of the hypothesis.

6.7.2 Statistical Methods and Tests

The approximate entropy for each of the measured time series was compared to the approximate entropy of a control noise signal. The isoflurane and enflurane measured time series were treated as separate groups, and each was individually compared to the noise signal control group.

A Student's T-test was used to compare the measured and the control groups, with, as stipulated in chapter 3, a p value of <0.05 being considered significant.

6.7.3 Results

	APPROXIMATE ENTROPY
T-test isoflurane group	0.000499
T-test enflurane group	0.003085

Table 6-4 Results of Student's T-test for the measured time series and the noise control signals

All the Student's T-test comparisons yielded p values of < 0.05. These results strongly recommend the acceptance of the null hypothesis stated above(6.7.1) and more specifically, add to the evidence presented in chapter 5 that there is a fractal attractor underlying the measured time series for both isoflurane and enflurane.

6.7.4 Power Analysis

To prevent a type II statistical error from being made, where the null hypothesis is accepted when the hypothesis is actually true, a power analysis[11] was performed. For the analysis, an alpha level of 2.35 was used which corresponds to a p value of <0.01 for the rejection of the null hypothesis. A power level of >0.8 was considered acceptable[11].

6.7.4.1 Power Analysis of the isoflurane group

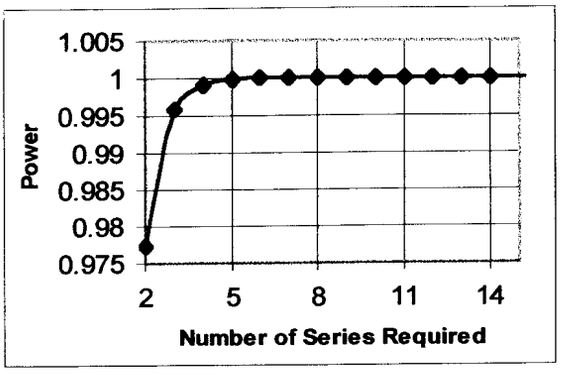

Figure 6-1 Power of the Student's T-test for the isoflurane measured time series

6.7.4.2 Power analysis of the enflurane group

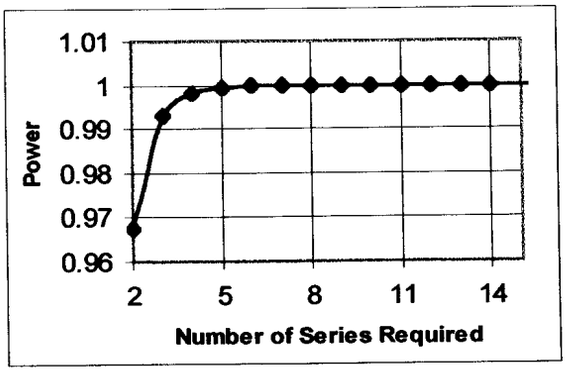

Figure 6-2 Power of the Student's T-test for the enflurane measured time series

6.7.4.3 Power Analysis conclusion

Twenty series were used in each of the Student's T-test analyses. All the power analysis showed that this was more than adequate for a power of > 0.8 and a p value of < 0.01.

6.8 Conclusion

The results presented above are further evidence for a fractal attractor underlying the absorption of both isoflurane and enflurane. These results reach statistical significance ($p<0.05$) with acceptable statistical power (>0.8).

6.9 References

[1] Pincus S.M.,Goldberger A.L., Physiological Time-Series Analysis: What Does Regulatory Quantify? American Journal Of Physiology 1994:266;H1643-H1656.

[2] Aarimaa T.R.,Oja K.A.,Valimaki I. Interaction Of Heart Rate And Respiration In Newborn Babies. Pediatric Research 1988:24;745-750.

[3] Kluge K.A.,Harper R.M.,Schechtman V.L.,Wilson A.J.,Hoffman H.J., Southall D.P. Spectral Analysis Assessment Of Respiratory Sinus Arrithymia In Normal And Infants Who Subsequently Died Of Sudden Infant Death Syndrome. Pediatric Research 1988:24;677-682.

[4] Goldberger A.L.,West B.J. Fractals In Physiology And Medicine. Yale Journal Of Biology And Medicine 1987:60;421-435.

[5] Grassberger P.,Procaccia I. Estimation Of The Kolmogorov Entropy From A Chaotic Signal. Physiology Review 1983:A28;2591-2593.

[6] Eckmann J.P.,Ruelle D. Ergodic Theory Of Chaos And Strange Attractors. Review Of Modern Physiology 1985:57;617-656.

[7] Moon C.M. Chaotic And Fractal Dynamics. An Introduction For Applied Scientists And Engineers. John Wiley And Sons 1992.

[8] Wolf A.,Swift J.B.,Swinney H.L.,Vastano J.A. Determining Lyapunov Exponents From A Time Series. Physica D 1985:16D;285-317.

[9] Jacobson R. Microsoft Excel 97 Visual Basic Step By Step. Microsoft Press 1997.

[10] Cerutti S.,Carrault G.,Cluitmans P.J.M.,Kinie A.,Lipping T.,Nikolaidis N.,Pitas I., Signorini M.G. Non-Linear Algorithms For Processing Biological Signals. Computer Methods And Programs In Biomedicine 1996:51;51-73.

[11] Steyn A.G.W.,Smit C.F.,Du Toit S.H.C., Strasheim C. Modern Statistics In Practice. JL Van Schaik 1996

7 Lyapunov exponents

7.1 Definition

Lyapunov exponents are the average exponential rates of divergence or convergence of nearby orbits in phase space[1]. The calculation of Lyapunov exponents is a tool for determining whether or not a system is chaotic[2], and quantifying the sensitive dependence on initial conditions.

7.2 Discussion

7.2.1 General description

Since nearby orbits correspond to nearly identical states, exponential orbital divergence means that systems whose initial differences may not be resolvable, will soon behave differently, and predictability will soon be lost. Any system containing at least one positive Lyapunov exponent is defined to be chaotic[1,3]. The magnitude of the exponent reflects the time scale on which the dynamics of the system become unpredictable.

Assuming two trajectories $a_1(t)$ and $a_2(t)$ are starting with a small difference (i.e., a small distance in phase space), for the distance Δ the following relation holds[3]:

$$\Delta(t) = |a_2(t) - a_1(t)| = |a_2(0) - a_1(0)| \cdot \exp(\lambda t) = \varepsilon \cdot \exp(\lambda t)$$

The first exponent has to be positive for the system to be chaotic, but the following one may be positive or negative[4]. The sum of the Lyapunov exponents is the timer-averaged divergence of the phase space velocity, and is therefore a quantitative measure for chaotic behavoir[3]. A dissipative dynamical system will have at least one negative exponent[1]. A Lyapunov exponent of zero holds for a periodic system[3].

The magnitudes of the Lyapunov exponents quantify an attractor's dynamics in information theoretic terms. The exponents measure the rate at which the system process creates or destroys information[1]. Thus the

exponents are expressed in bits of information per second or bits per orbit for a continuous system and bits per iteration for a discrete system.

7.2.2 Implementation details

7.2.2.1 Selection of embedding dimension and delay time

In principle, when using delay coordinates to reconstruct an attractor, an embedding dimension, m, of the original attractor is obtained for a sufficiently large m and almost any choice of the time delay, τ. Accurate exponent estimation requires some care in choosing these two parametes[1,5]. An embedding is usually obtained if m is chosen to be greater than twice the dimension of the underlying attractor, although using smaller values of m may often yield reliable Lyapunov exponents[1]. When an attractor is reconstructed in phase space, whose dimension is too low, "catastrophes" or so called spurious exponents the interleave a distinct part of the attractor are likely to result[5]. If m is chosen too large, noise will tend to decrease the density of the points defining the attractor, making it hard to find replacement points. Increasing m past what is minimally required has the effect of unnecessarily increasing the level of contamination of the data[1].

7.2.2.2 Noise

Noise in an infinite dimension process that, unlike the deterministic component of the data, fills each available phase space dimension in reconstructing the attractor. Noise can originate either in measurement because of simple lack of resolution, or form fluctuations in the state of the system or its parameters, which enter into the dynamics. It is ironic that noise is not a problem unless large amounts of data are available to define the attractor. This is because noise is only detectable when the point density is high enough to provide replacements near the noise length scale[1].

Low pass filtering has been proposed as an approach for reducing the effects of noise[1]. As could be expected filtering can distort shapes in the attractor, but the divergent nature of the attractor is not usually lost.

Published figures estimate about 20 percent difference in Lyapunov exponent estimation for filtered and unfiltered experimental data[1].

7.3 Computation algorithms

The main idea in calculating the Lyapunov exponent is comparing an orbit belonging to some initial condition with an orbit for an initial condition, which carries and error E_0. Then it is possible to record how the error amplifies during the course of the iteration to $E_1, E_2, \ldots$. The error amplification factor $|E_n/E_0|$ is written as a "telescope product"[6].

$$\left|\frac{E_n}{E}\right| = \left|\frac{E_n}{E_{n-1}}\right|\left|\frac{E_{n-1}}{E_{n-2}}\right|\cdots\left|\frac{E_1}{E_0}\right|$$

The Lyapunov exponent characterizes the average logarithmic growth of the relative error per iteration. To arrive at a well-defined exponent, the size of the initial error must approach zero. In practice the size of the error in each iteration is renormalized to some convenient number $\in$[6].

$$\lambda = \lim_{n\to\infty}\lim_{E0\to 0}\frac{1}{n}\sum_{k=1}^{n}\log\left|\frac{E_k}{E_{k-1}}\right|$$

The choice of the size of the error $\in$ to which is renormalized after each iteration may effect the result. The amplification factor for infinitesimally small errors, is obtained when $\in\to 0$. Using a derivative transformation, it is possible to compute how much an infinitesimally small error in a point (x,y) of the attractor is transformed by one iteration[6].

$$DH(x,y) = \begin{pmatrix} -2ax & 1 \\ b & 0 \end{pmatrix}$$

If the error is in the direction of the given vector (dx,dy), then this vector can be multiplied by the derivative matrix[6].

$$\begin{pmatrix} -2ax & 1 \\ b & 0 \end{pmatrix}\begin{pmatrix} dx \\ dy \end{pmatrix} = \begin{pmatrix} -2ax\cdot dx + dy \\ b\cdot dx \end{pmatrix}$$

The amplification factor is determined by the quotient of the lengths of the two vectors (dx, dy) and $(-2ax \cdot dx + dy, b \cdot dx)$.

Using this approach the algorithm may be summarized as follows[6]:

7.3.1 Initialization

Iterate the initial point $(0,0)$ one hundred times to arrive at (x,y). initialize an accumulator to zero.

7.3.2 Initial error

For an arbitrary angle ϕ, consider $(\cos\phi, \sin\phi)$, the direction of the error.

7.3.3 Transformation

Compute the transformed error according to

$$\begin{pmatrix} -2ax & 1 \\ b & 0 \end{pmatrix} \begin{pmatrix} dx \\ dy \end{pmatrix} = \begin{pmatrix} -2ax \cdot dx + dy \\ b \cdot dx \end{pmatrix}$$

Then iterate (x,y), i.e. obtain the point $H(x,y)$ and the transformed error

$(-2ax \cdot \cos\phi + \sin\phi, b \cdot \cos\phi)$.

7.3.4 Error amplification

The error has increased (or decreased) by the factor

$$d = \sqrt{(-2ax \cdot \cos\phi + \sin\phi)^2 + (b \cdot \cos\phi)^2}$$

Accumulate the logarithm of this factor.

7.3.5 Renormalization

Replace the old point (x,y) by its successor $H(x,y)$ and replace the old error direction by the new directional vector $(\cos\phi, \sin\phi)$ by $(-x \cdot \cos\phi + \sin\phi, b \cdot \cos\phi)/d$.

7.3.6 Loop

Go back to step 3, transformation until N iterations have been performed.

7.3.7 Result

Divide the contents of the accumulator by N.

7.4 Summary of the main aspects of Lyapunov exponents relevant to strange attractors

- It is recognized that an attractor is chaotic if it has one positive Lyapunov exponent .
- In discrete systems, as well as in continuous systems, there are as many Lyapunov exponents as there are dimensions of underlying space.
- The sum of all Lyapunov exponents characterizes how fast area (in two dimensions) or volume (in three dimensions) expands or shrinks.
- The Lyapunov exponents are independent of the choice of coordinates.

7.5 Program used to estimate the Lyapunov exponents

The program SANTIS has the capability to estimate Lyapunov exponents for a time series[7].

7.5.1 Testing the program

7.5.1.1 Method

The program used was tested to see if it could measure the Lyapunov exponents accurately. The null hypothesis was that is unable to distinguish known chaos from noise. A Henon time series and Logistic map

with a starting value 0.2 and a delta value of 3.8 were used as known chaotic series[2]. (These two time series may be found in Appendix E). Four noise series generated by SANTIS were used as control series (These four time series may be found in Appendix D). The Student's T-test was used as the test statistic and a p value of <0.05 was considered significant, in order to reject the null hypothesis.

7.5.1.2 Results

	HENON	LOGISTIC MAP	NOISE1	NOISE2	NOISE3	NOISE 4	P
Lyapunov exponent	3.90	4.69	0.22	0.22	0.22	0.26	0.000074
Settings for the Lyapunov exponent Calculation with SANTIS							
Delay / tau	1	1	1	1	1	1	
Embedding dimension	2	2	2	2	2	2	
Minimum Distance of Trajectories (% of sample range)	1.0	1.0	1.0	1.0	1.0	1.0	
Maximum Distance of Trjectories (% of sample range)	10.0	10.0	10.0	10.0	10.0	10.0	

Table 7-1 Lyapunov exponents for known chaos and known noise signals

The calculated p value was 0.000074. This is less than 0.05 and therefore the null hypothesis is rejected and it is concluded that the program is successfully able to differentiate known chaos from known noise.

7.6 Lyapunov exponents for the time series measured

The Lyapunov exponents were calculated in the same manner for the twenty measured time series. The time series are to be found in Appendix B.

FILE NAME	LYAPUNOV EXPONENT	DELAY / TAU	EMBEDDING DIMENSION	MINIMUM DISTANCE OF TRAJECTORIES (% OF SAMPLE RANGE)	MAXIMUM DISTANCE OF TRJECTORIES (% OF SAMPLE RANGE)
Iso-01	0.79	1	2	1	10
Iso-02	1.27	1	2	1	10
Iso-03	0.207	1	2	1	10
Iso-04	1.63	1	2	1	10
Iso-05	1.107	1	2	1	10
Iso-06	0.638	1	2	1	10
Iso-07	0.41	1	2	1	10
Iso-08	1.06	1	2	1	10
Iso-09	1.66	1	2	1	10
Iso-10	0.65	1	2	1	10
Enf-01	0.645	1	2	1	10
Enf-02	0.131	1	2	1	10
Enf-03	0.687	1	2	1	10
Enf-04	1.245	1	2	1	10
Enf-05	0.393	1	2	1	10
Enf-06	0.579	1	2	1	10
Enf-07	0.52	1	2	1	10
Enf-08	0.452	1	2	1	10
Enf-09	0.37	1	2	1	10
Enf-10	0.519	1	2	1	10

Table 7-2 Lyapunov exponents for the measured time series

7.7 Lyapunov exponents for the Control Noise Signals

NOISE NEW	LYAPUNOV EXPONENT
1	0.123468
2	0.074407
3	0.126614
4	0.102054
5	0.100305
6	0.120309
7	0.098572
8	0.100782
9	0.098225
10	0.092514

Table 7-3 Lyapunov exponents of the control noise time series

7.8 Statistical Analysis

The hypothesis and null hypothesis were formulated and stated in chapter 3, and are repeated here for clarity sake.

7.8.1 Hypothesis

The absorption of isoflurane and enflurane is a non-linear process. To detect nonlinearity four conditions must be met:

- Fractal Dimension of the attractor
- Sensitivity to initial conditions
- Invariant probability distribution of the attractor
- Detection of an underlying dynamical process

7.8.1.1 Null hypothesis

The absorption of the anaesthetic agents Isoflurane and Enflurane is fully described by independent and identically distributed random variables, i.e. the variability seen in the absorption is random[8] and there is no underlying deterministic process.

The time series measured will be analytically indistinguishable from noise signals.

7.8.1.2 Sensitivity to initial conditions

This chapter is testing this part of the hypothesis.

7.8.2 Statistical Methods and Tests

The Lyapunov exponents for each of the measured time series was compared to the Lyapunov exponent a control noise signal. The isoflurane and enflurane measured time series were treated as separate groups and each was individually compared to the noise signal control group.

A Student's T-test was used to compare the measured and the control groups, with, as stipulated in chapter 3, a p value of <0.05 being considered significant.

7.8.3 Results

	LYAPUNOV EXPONENTS
T-test isoflurane group	0.000426
T-test enflurane group	0.000824

Table 7-4 Results of the Student's t-test comparisons for the two groups of measured time series

All the T-test comparisons yielded p values of < 0.05. These results strongly recommend the acceptance of the null hypothesis stated above (7.8.1) and more specifically, that there is evidence for sensitivity to initial conditions underlying the measured time series for both isoflurane and enflurane.

7.8.4 Power Analysis

To prevent a type II statistical error from being made, where the null hypothesis is accepted when the hypothesis is actually true, a power analysis[9] was performed. For the analysis, an alpha level of 2.35 was used which corresponds to a p value of <0.01 for the rejection of the null hypothesis. A power level of >0.8 was considered acceptable[9].

7.8.4.1 Power analysis for Isoflurane group

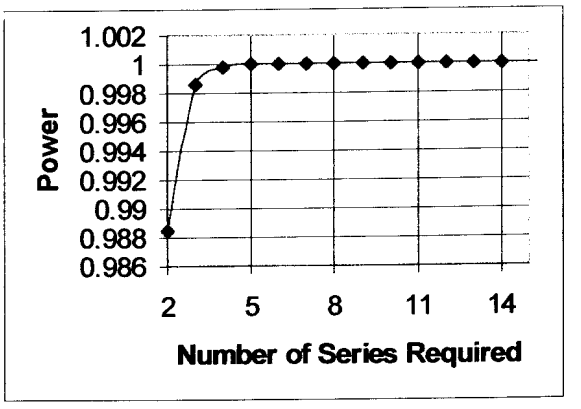

Figure 7-1 Power of the Student's T-test for the isoflurane measured time series

7.8.4.2 Power analysis of the enflurane group

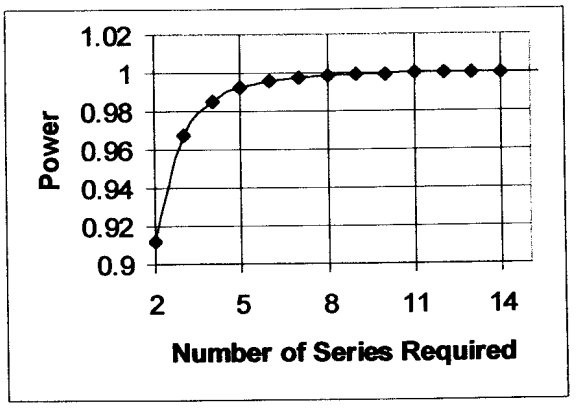

Figure 7-2 Power of the Student's T-test for the enflurane measured time series

7.8.4.3 Power analysis conclusion

Twenty series were used in each of the Student's T-test analyses. All the power analysis showed that this was more than adequate for a power of > 0.80 and a p value of < 0.01.

7.9 Conclusion

The results presented above show that there is evidence for sensitivity to initial conditions underlying the absorption of both isoflurane and enflurane. These results reach statistical significance ($p<0.05$) with acceptable statistical power (>0.8).

7.10 References

[1] Wolf A.,Swift J.B.,Swinney H.L.,Vastano J.A. Determining Lyapunov Exponents From A Time Series. Physica D 1985:16D;285-317.

[2] Moon F.C. Chaotic And Fractal Dynamics: An Introduction For Applied Scientists And Engineers. John Wiley And Sons 1992.

[3] Persson P.B.,Wagner C.D. General Principles Of Chaotic Dynamics. Cardiovascular Research 1996:31;332-341.

[4] Mansier P.,Clairambault J.,Charlotte N.,Medigue C.,Vermeiren C.,Lepape G.,Carre F.,Gouranropoulou A.,Swyndghauw B. Linear And Non-Linear Analysis Of Heart Rate Variability: A Mini Review. Cardiovascular Research 1996:31;371-379.

[5] Cerutti S.,Carrault G.,Cluitmans P.J.M.,Kinie A.,Lipping T.,Nikolaidis N.,Pitas I.,Sigorimi M.G. Non-Linear Algorithms For Processing Biological Signals. Computer Methods And Programs In Biomedicine. 1996:51;51-73.

[6] Pietgen H.,Jurger H.,Saupe D. Chaos And Fractals: New Frontiers Of Science. Springer Verlag 1992.

[7] Vanderhouten R.,Rasche M.,Tegtmeier H.,Goebbels G. SANTIS User Manual. Institute Of Physiology, University Of Aachen 1996.

[8] Cerutti S.,Carrault G.,Cluitmans P.J.M.,Kinie A.,Lipping T.,Nikolaidis N.,Pitas I., Signorini M.G. Non-Linear Algorithms For

Processing Biological Signals. Computer Methods And Programs In Biomedicine 1996:51;51-73.

[9] Steyn A.G.W.,Smit C.F.,Du Toit S.H.C., Strasheim C. Modern Statistics In Practice. JL Van Schaik 1996

8 The Method of Surrogate Data

8.1 Definition

The method of surrogate data is a statistical approach to identifying nonlinearity in a time series. The method first specifies some linear process as a null hypothesis, then generates surrogate data sets which are consistent with this null hypothesis, and finally computes a discriminating statistic for the original and for each of the surrogate data sets. If the value computed for the original data is significantly different than the ensemble of values computed for the surrogate data, then the null hypothesis is rejected, and nonlinearity is detected[1].

8.2 Discussion

8.2.1 Introduction

The inverse problem for a nonlinear system is to determine the underlying dynamical process in the practical situation where all that is available is a time series of data. For experimental sets simple autocorrelation and Lyapunov exponent estimates can signal chaos where there is none. This is particularly so of data sets that are short and noisy[1]. Most authors recognize these pitfalls, but they are not easily avoided.

Some data sets very cleanly exhibit low dimensional chaos, but there are many examples where the evidence is sketchy and difficult to evaluate. The real complication arises because low dimensional chaos and uncorrelated noise are not the only available alternatives. The erratic fluctuations that are observed in an experimental time series owe their dynamical variation to a number of various influences. Chaos, nonchaotic but still nonlinear determinism, linear correlations and noise, both in the dynamics and in the measuring apparatus[1,2,3].

The goal of identifying linearity is considerably easier than that of positively identifying chaotic dynamics. The approach of surrogate data is to specify a well defined underlying linear process or null hypothesis, and to

determine the distribution of the quantity, for example, dimension, for an ensemble of surrogate data sets which are just different realizations of the hypothesized linear stochastic process[1,4].

Error bars can be put on the value given by the surrogates reliably because of the many realizations of the null hypothesis, the errors can be estimated numerically form the standard deviation of all the estimated dimensions of the surrogate data sets[1].

8.2.2 Statistical Hypothesis testing

The formal application of the surrogate data method is expressed statistically using a null hypothesis against which observations are tested, and a discriminating statistic[1].

The null hypothesis is a potential explanation that is sought to be shown inadequate for explaining the data. The discriminating statistic is a number, which quantifies some aspect of the time series. If this number is different for the observed data, than would be expected under the null hypothesis, then the null hypothesis can be rejected[1].

An ensemble of surrogate data sets are generated which share given properties of the observed times series. These are, for example, mean variance, and Fourier spectrum. Nevertheless, these surrogate data sets are otherwise random as specified by the null hypothesis[4]. For each surrogate data set, the discriminating statistic is computed, and form this ensemble of statistics the distribution is approximated[1].

This approach is computationally intensive, but avoids analytical deviation, which can be difficult, if not impossible. This allows increased flexibility in the choice of the null hypothesis and the discriminating statistic(s). The hypothesis and statistic can even be chosen independently of each other[1].

8.2.3 Computing significance

Let Q_D denote the statistic computed for the original time series and Q_{Hi} for the *i*-th surrogate generated under the null hypothesis. Let μ_H and σ_H denotes the sample mean and the standard deviation of the distribution of Q_H [1].

If multiple realizations of the experimental data are available, then it may be possible to compare the two data sets directly using a Mann-Whitney or a student-t test. Alternatively if only one realization of the experimental data is available, the following method can be used[1].

The measure of "significance" is defined by the difference between the original and the mean surrogate value of the statistic, divided by the standard deviation of the surrogate data values.

$$\vartheta = \frac{|Q_D - \mu_H|}{\sigma_H}$$

The significance is a dimensionless quantity, but is call by convention, "sigmas"[1].

8.2.4 Estimating error bars on significance

The errors are computed by the standard propagation of errors methodology. They are written on the graph as $\Delta\vartheta$.

$$\left(\frac{\Delta\vartheta}{\vartheta}\right)^2 = \left(\frac{\Delta|\mu_H - \mu_D|}{\mu_H - \mu_D}\right)^2 + \left(\frac{\Delta\sigma_H}{\sigma_H}\right)^2$$

$$= \frac{(\Delta\mu_H)^2 + (\Delta\mu_D)^2}{(\mu_H - \mu_D)^2} + \left(\frac{\Delta\sigma_H}{\sigma_H}\right)^2$$

Now the error of the sample mean based on *N* observations is given by $(\Delta\mu)^2=\sigma^2/N$, and the error of the sample standard deviation is $(\Delta\sigma)^2=\sigma^2/N$.

Therefore[1]:

$$\left(\frac{\Delta\vartheta}{\vartheta}\right)=\frac{\sigma_H^2/N_H+\sigma_D^2/N_D}{(\mu_H-\mu_D)^2}+\frac{1}{2N_H}$$

The absolute error is given by [1]:

$$\Delta\vartheta=\sqrt{\left(1+\frac{1}{2}\vartheta^2\right)/N_H+(\sigma_D/\sigma_H)^2/N_D}$$

When only a single realization of the time series is available, then σ_D is taken to be zero and the second term of the equation is ignored.

8.2.5 Battery of discriminating statistics

The method of surrogate data can in principle be used with virtually any discriminatory statistic. Formally the null hypothesis can be rejected if the statistic has different distributions for the data and the surrogates. However the method is more useful if the statistic actually provides a good estimate of a physically interesting quantity[1]. Choices of statistics used have included correlation dimension, Lyapunov exponents, forecasting error and correlation integral[1,5].

8.3 Algorithms for generating surrogate data

8.3.1 Unwindowed Fourier Transform Algorithm

This algorithm is based on the null hypothesis that the data came from a linear Gaussian process. The surrogate data are constructed to have the same Fourier spectra as the raw data[1].

First the Fourier transform is computed for both positive and negative frequencies, $f=0,1/N,2/N,....1/2$, without the benefit of windowing. The Fourier transform has complex amplitude at each frequency. To randomize the phases, each complex amplitude is multiplied by $e^{i\phi}$, where ϕ is independently chosen for each frequency in the interval $[0,2\pi r]$. in order for the inverse Fourier transform to be real, i.e. with no imaginary

components, the phases must be symmetrized, so that $\phi(f)=-\phi(-f)$. Finally, the inverse Fourier transform is the surrogate data[1].

This algorithm has at least two limitations. Firstly that it does not reproduce " pure" frequencies very well. Secondly spurious high frequencies can be introduced, most probably as an artifact of the Fourier transform, which assumes the time series is periodic with a period of N[1].

8.3.2 Windowed Fourier Transform Algorithm

The problem of spurious high frequencies can be addressed by windowing the data before taking the Fourier transform. The time series is multiplied by a function $w(f)=sin(\pi t/N)$ which vanishes at the end points $t=0$ and $t=N$. This suppresses the jump discontinuity from the last to the first point, and seems to effectively get rid of the high frequency effect. It may however introduce spurious low frequencies form the power spectrum $w(t)$ itself[1].

8.3.3 Amplitude Adjusted Fourier Transform

This algorithm generates a surrogate data set associated with the null hypothesis that the observed time series is a monotonic nonlinear transformation of a linear gaussian process[1]. The idea is to first rescale the values in the original time series so that they are gaussian. Then the windowed or unwindowed Fourier transformation algorithms are used to make a surrogate time series, which has the same Fourier spectrum as the rescaled data. Finally, the gaussian surrogate is then rescaled back to have the same amplitude distribution as the original time series.

8.4 Experimental observations using this technique

The method of surrogate data has been applied to both experimental and other data. Some of the observations made were[1]:

a) Increasing the number of points in a time series increases the significance with which nonlinearity can be detected in a time series, which is known to be chaotic.

b) Increasing the complexity of the chaotic time series decreases the ability to distinguish from linearity.

c) Nonlinearity could be detected even with a signal to noise ratio of one to one, using a time series of length 512.

d) The decrease in significance is not always monotonic, low levels of dynamical noise can make the nonlinearity more evident.

e) Oversampling can produce artifacts of autocorrelation and mask nonlinearity, which is evident if a correct sampling interval is used.

8.5 Program used

The public domain program SANTIS has the capacity for generating Surrogate Data[6] using a random phase method, which is described in 8.3.1. This algorithm is based on the null hypothesis that the data came from a linear Gaussian process[1].

8.5.1 Testing the program

8.5.1.1 Method

8.5.1.1.1 Statistical Tests

The program used was tested to see if it generated surrogate data accurately. The null hypothesis tested against was that is unable to distinguish known chaos from noise. A Henon time series was used as a known chaotic series[7]. This time series may be found in Appendix E. A noise signal generated by SANTIS was used as a control series. (This time series may be found in Appendix D).

For the present situation where only one realization of the 'experimental' data is available, a modified T-test is used to calculate a measure of significance[1]. The measure of significance (S) is defined by the difference between the original and the mean surrogate value of the statistic, divided by the standard deviation of the surrogate values:

$$S = \frac{|Q_D - \mu_H|}{\sigma_H}$$

Where Q_D denotes the statistic computed for the original time series, μ_H is the sample mean and σ_H is the sample standard deviation. The significance is properly a dimensionless quantity. If the distribution of the statistic is gaussian (and numerical experiments indicate that this is often a reasonable approximation[1]), then the p value is given by p=P($Z \geq S/\sqrt{2}$)[1], where Z has a n(0,1) distribution[8]. This gives the probability of observing significance S or larger if the null hypothesis is true. For the current test, a p value of <0.05 was considered significant, in order to reject the null hypothesis.

8.5.1.2 Results

HENON TIME SERIES	LYAPUNOV EXPONENT	CORRELATION DIMENSION
Henon Original	2.07854	1.24500
SD1	1.34043	3.02000
SD2	1.15344	3.05000
SD3	1.33218	3.15000
SD4	1.36878	2.96000
SD5	1.33900	3.06000
Mean of Surrogates	1.30676	3.04800
Standard deviation of Surrogates	0.08685	0.06907
NOISE TIME SERIES	LYAPUNOV EXPONENT	CORRELATION DIMENSION
Noise Original	0.12347	3.03000
SD1	0.13290	2.93500
SD2	0.12597	3.03200
SD3	0.14202	2.99490
SD4	0.12780	2.95600
SD5	0.13647	3.14750
Mean of Surrogates	0.13303	3.01308
Standard deviation of Surrogates	0.00652	0.08383

Table 8-1 Calculated values for the henon and noise time series

	LYAPUNOV EXPONENT		CORRELATION DIMENSION	
	Sigma	p	Sigma	p
Henon Time Series	8.886	1.66E-10	26.1057	→0
Noise Times Series	1.4668	0.149	0.20183	0.4432

Table 8-2 Calculated statistics for the henon and noise time series and their surrogates

The *p* values for the known chaotic signal, the Henon Time series, and its surrogates for both the Lyapunov exponent and the correlation dimension are well below 0.05. The *p* values for the known noise series and its surrogates are well above 0.05. It is therefore concluded that the SANTIS program is able to distinguish noise from known chaos using the method of surrogate data The surrogate data sets for the Henon Time series and the Noise time series are to be found in Appendix C.

8.6 The Method of Surrogate Data applied to the time series measured

8.6.1 Hypothesis

The absorption of isoflurane and enflurane is a non-linear process. To detect nonlinearity four conditions must be met:

- Fractal Dimension of the attractor
- Sensitivity to initial conditions
- Invariant probability distribution of the attractor
- Detection of an underlying dynamical process

8.6.1.1 Null hypothesis

The absorption of the anaesthetic agents Isoflurane and Enflurane is fully described by independent and identically distributed random variables, i.e. the variability seen in the absorption is random[9] and there is no underlying deterministic process.

The time series measured will be analytically indistinguishable from noise signals.

8.6.1.2 Invariant probability distribution of the attractor

This part of the hypothesis is being tested by this chapter.

8.6.2 Statistical Methods and Tests and Data processing

The twenty measured time series were processed using SANTIS and a surrogate data set for each time series was constructed. A single surrogate was made for each series because they are multiple realizations of observational data[1]. The surrogate data sets are to be found in Appendix J. The statistics chosen for the analysis were the correlation dimension and the Lyapunov exponent[1]. These two statistics were calculated for the surrogates and the originals as set out in Chapters 5 and 7 respectively.

The isoflurane group and the enflurane group are each compared to their own surrogate data set. The two groups of statistics will be compared using a Student's T-test[1] and a p value of < 0.05 will be considered significant.

8.6.3 Power Analysis

To prevent a type II statistical error from being made, where the null hypothesis is accepted when the hypothesis is actually true, a power analysis[8] was performed. For the analysis, an alpha level of 2.35 was used which corresponds to a p value of < 0.01, for the rejection of the null hypothesis. A power level of >0.8 was considered acceptable[8].

8.6.3.1 Power Analysis for the Isoflurane Group

8.6.3.1.1 Lyapunov Exponent

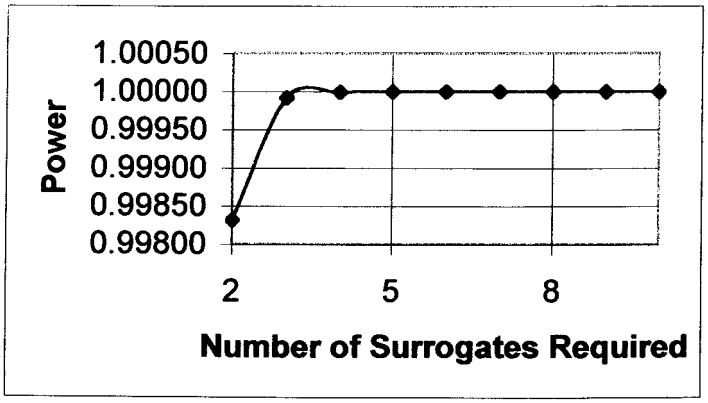

Figure 8-1 Power of the Student's T-test for the isoflurane surrogates

8.6.3.1.2 Correlation Dimension

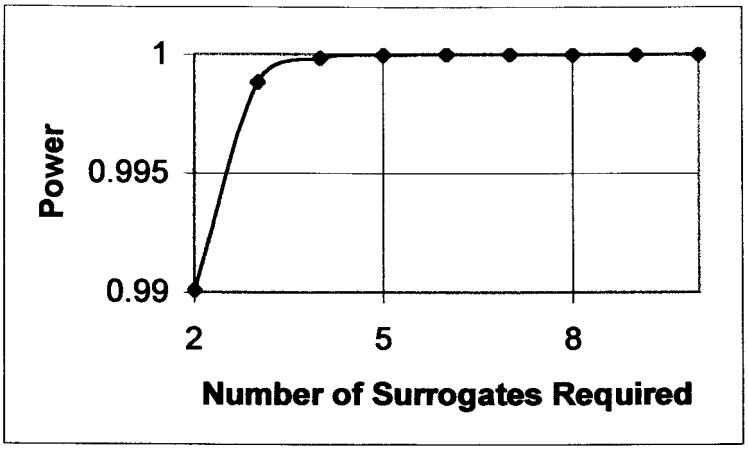

Figure 8-2 Power of the Student's T-test for the isoflurane surrogates

8.6.3.2 Power Analysis for the Enflurane Group

8.6.3.2.1 Lyapunov Exponent

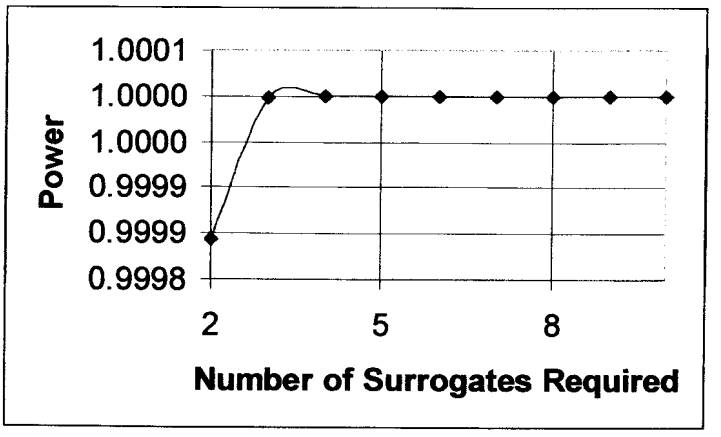

Figure 8-3 Power of the Student's T-test for the enflurane surrogates

8.6.3.2.2 Correlation dimension

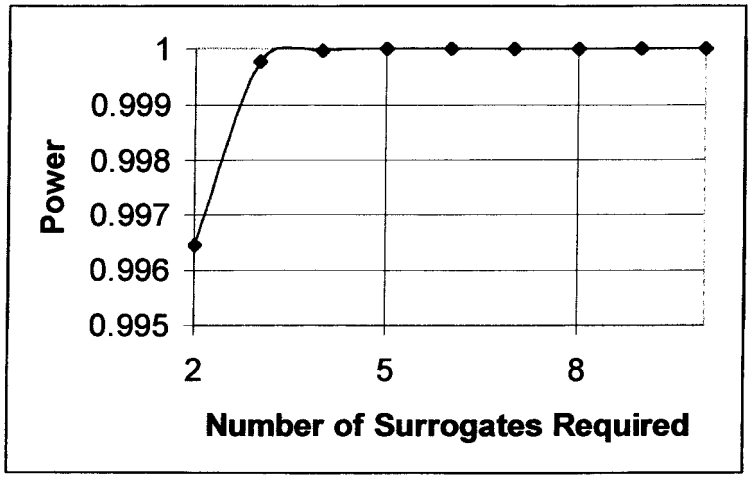

Figure 8-4 Power of the Student's T-test for the enflurane surrogates

8.6.3.3 Power Analysis conclusion

Ten surrogates were used in each of the Student's T-test analyses. All the power analysis showed that this was more than adequate for a power of > 0.8 and a p value of < 0.01.

8.6.4 Results

8.6.4.1 Tabular summary of results obtained

ORIGINALS			SURROGATES	
	Lyapunov Exponent	Correlation Dimension	Lyapunov Exponent	Correlation Dimension
Iso-01	0.79	0.785141	0.95	2.54573
Iso-02	1.27	1.48417	1.77	2.63195
Iso-03	0.207	0.952904	2.71	2.70931
Iso-04	1.63	1.03614	1.57	2.28634
Iso-05	1.107	1.50338	1.76	2.84977
Iso-06	0.638	1.3673	1.79	2.50964
Iso-07	0.41	1.04189	1.59	2.45525
Iso-08	1.06	1.36093	2.38	2.54241
Iso-09	1.66	1.52047	0	2.70942
Iso-10	0.65	1.57578	1.86	2.42537
Student's T-test	0.378105	0.0000001	(p Values)	

Table 8-3 The results for the measured isoflurane times series and their surrogates

ORIGINALS			SURROGATES	
	Lyapunov Exponent	Correlation Dimension	Lyapunov Exponent	Correlation Dimension
Enf-01	0.645	1.88901	2.11	2.61761
Enf-02	0.131	0.814319	2.07	2.48397
Enf-03	0.687	0.975127	1.87	2.55907
Enf-04	1.245	1.81347	1.358	2.51946
Enf-05	0.393	0.0982057	2.38	2.87178
Enf-06	0.579	1.46198	2.995	2.92315
Enf-07	0.52	1.46198	1.922	2.92315
Enf-08	0.452	1.23643	2.32	3.22789
Enf-09	0.37	0.101749	2.17	2.96908
Enf-10	0.519	0.80455	1.967	2.63558
Student's T-test	0.0000119	0.0000187	(p values)	

Table 8-4 The results for the measured enflurane times series and their surrogates

8.6.4.2 Conclusion

The results presented above show that there is evidence for an invariant probability distribution of the attractor underlying the absorption of both isoflurane and enflurane. These results all reach statistical significance ($p < 0.05$) with acceptable statistical power (>0.8).

8.7 References

[1] Theiler J.,Eubank S.,Longtin A.,Galdrikian B.,Farmer J.D. Testing For Nonlinearity In A Time Series: The Method Of Surrogate Data. Physica D 1992:58;77-94.

[2] Datex AS-3 Anaesthesia Monitor Operators Manaul. Datex Division, Instumentation Corporation, Helskinki, Finland. 1995:2-21.

[3] Datex Capnomac Ultima Anaesthesia Monitor Operators Manual. Datex Division, Instrumentaion Corporation, Helsinki, Finland. 1994:14-3.

[4] Elbert T.,Ray W.J.,Kowalik Z.J.,Skinner J.E.,Graf K.E.,Birbaumer N. Chaos And Physiology: Determenistic Chaos In Excitable Cell Assemblies. Physiological Reviews 1994:74;1-47.

[5] Kanters J.K.,Holstein-Rathlou N.H.,Agner E. Lack Of Evidence For Low-Dimensional Chaos In Heart Rate Variability. Journal Of Cardiovascular Electrophysiology 1994:5;591-601.

[6] Vanderhouten R.,Rasche M.,Tegtmeier H.,Goebbels G. SANTIS User Manual. Institute Of Physiology, University Of Aachen 1996.

[7] Moon C.M. Chaotic And Fractal Dynamics. An Introduction For Applied Scientists And Engineers. John Wiley And Sons 1992.

[8] Steyn A.G.W.,Smit C.F.,Du Toit S.H.C.,Strasheimc. Modern Statistics In Practice. J.L. Van Schaik 1996.

[9] Cerutti S.,Carrault G.,Cluitmans P.J.M.,Kinie A.,Lipping T.,Nikolaidis N.,Pitas I., Signorini M.G. Non-Linear Algorithms For Processing Biological Signals. Computer Methods And Programs In Biomedicine 1996:51;51-73.

9 Nonlinear forecasting

9.1 Definition

Nonlinear forecasting is an approach for making short term predictions about the trajectories of chaotic dynamical system. It distinguishes apparent noise associated with deterministic chaos from sampling error and other sources of externally induced environmental noise[1,2].

9.2 Discussion

Nonlinear forecasting combines some new ideas with previously described techniques to make short term predictions that are based on a library of past patterns in the time series[1,2]. By comparing the predicted and actual trajectories, tentative distinctions between dynamical chaos and measurement error can be made.

For a chaotic time series, the accuracy of nonlinear forecasting falls off with an increase in prediction interval, whereas for uncorrelated noise, the forecasting accuracy is roughly independent of the prediction interval[1]. The rate at which the prediction accuracy falls off for a chaotic time series gives an estimate of its Lyapunov exponent[3]. This method provides an estimate of the number of dimensions or "active variables" of the attractor underlying a time series that is identified as chaotic. It does not require a large number of data points, and seem to be useful when the observed time series has relatively few points.

9.2.1 Forecasting for a chaotic time series

Nonadjacent values in chaotic time series are completely uncorrelated, and standard statistical methods cannot be used to generate predictions two or more steps into the future that are significantly better than the mean value for the series. But if deterministic laws govern the system, then, even if the dynamical behavior is chaotic, the future may be

able to some extent be predictable from the behavior of past values that are similar to those of the present[1].

The predictions are sensitive to the choice of the embedding dimension, E[1]. They are less accurate with higher embedding dimensions. This effect is thought to be caused by the contamination of nearby points in the higher dimensional embeddings with points whose earlier coordinates are close but, whose recent and therefore more relevant coordinates are distant.

The forecasting technique is phenomenological in that it attempt to asses the qualitative character of a system's dynamics without attempting to provide an understanding of the physical or biological mechanisms which ultimately govern the system[1]. This contrasts strongly with many laboratory and field experiments, which often attempt to elucidate detailed mechanisms.

The time series is split into two parts and inferences are made about the dynamical nature of the system. This is done by examining the way in which the correlation coefficient between the predicted and the observed results for the second part of the times series varies with the prediction interval[1]. It has been shown to work with artificially generated time series, for which the underlying mechanisms are known, as well as for epidemiological data[1], heart rate analysis[2,4], action potential trains[3], the human EEG[5] and disease incidence[6].

9.3 Computational algorithm

First an embedding dimension, E, is chosen, and then lagged coordinates are used to represent each lagged sequence (with a lag time of τ) of data points, $\{x_t, x_{t-\tau}, x_{t-2\tau} \ldots x_{t-(E-1)\tau}\}$ as a point in E dimensional space. The results do not seem to be very sensitive to the choice of τ value, provided it is not too large[1]. Each sequence for which a prediction is to be made is now regarded as an E-dimensional point, comprising of its present value and the E-1 previous values each separated by one lag time τ. All nearby E

dimensional points are located in the state space, and a minimal neighborhood is defined to be such that the predictee is contained within the smallest simplex termed by its $E+1$ closest neighbors. The prediction is now obtained by projecting the domain of the simplex into its range, that is by keeping track of where the point in the simplex end up after p time steps. To obtain the predicted value, the original predictee position is computed within the range of its simplex, giving exponential weight to its original distances from the relevant neighbors[1].

Nonlinear forecasting is a non-parametric method which uses no prior information about the model used to generate the time series, only the information in the output itself[1,2].

9.4 *Program used*

Neither of the two programs used for analysis in this thesis have the facility to do the nonlinear forecasting method as described above.

Microsoft Excel 8® and Visual Basic for Applications® were used to develope a computer program using the algorithm outlined above. The code for the program is to be found in Appendix I.

9.4.1 Description

9.4.2 Testing the program

The program written was tested to see if it could perform nonlinear forecasting accurately. The null hypothesis is that it is unable to distinguish known chaos from noise. A Henon attractor time series as well as a noise series were used in the testing. The data for the Henon time series is to be found in Appendix E, the data for the noise series is to be found in Appendix D.

A Henon attractor time series of 1500 data points was used and the following results were obtained:

PREDICTION TIME	HENON	NOISE
	Correlation coefficient	Correlation coefficient
1	0.931009	0.508566
2	0.834199	0.446426
3	0.7625	0.522498
4	0.51392	0.429119
5	0.493131	0.482085
6	0.454723	0.484795
7	0.39385	0.472593
8	0.27307	0.508908
9	0.266334	0.403556
10	0.267688	0.436132

Table 9-1 Tabular results of non-linear forecasting with a henon attractor and a noise signal.

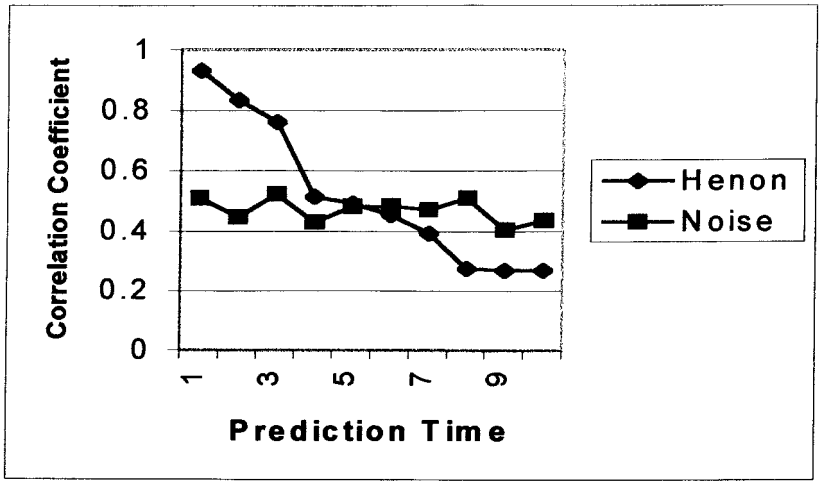

Figure 9-1 The correlation coefficient of the predicted and actual values for a henon attractor and a noise signal.

The decrease in the correlation coefficient with increasing prediction time is a characteristic of chaos when subjected to nonlinear prediction[1]. This property is noteworthy because it indicates a simple way to differentiate additive noise from deterministic chaos. Prediction with additive noise that is uncorrelated will seem to have a fixed amount of error, regardless of how far or close into the future one tries to project. However, prediction with deterministic chaos will tend to deteriorate as one tries to forecast into the future[1,4].

In this testing process, the noise signal serves as a control. It is therefore concluded that the program successfully distinguished two known chaotic signals from noise, and can therefore be used in the measured time series analysis.

9.5 Nonlinear forecasting applied to the measured time series

9.5.1 Tabular results of the nonlinear forecasting

	PREDICTION TIME									
Time Series	1	2	3	4	5	6	7	8	9	10
Iso-01	0.998405	0.998335	0.992936	0.992584	0.988504	0.985449	0.101956	0.941643	0.635765	0.504829
Iso-02	0.533014	0.600201	0.52655	0.518132	0.242406	0.247409	0.201772	0.253008	0.273863	0.242467
Iso-03	0.839198	0.564994	0.319887	0.279051	0.276087	0.384769	0.380413	0.32074	0.291326	0.219981
Iso-04	0.394032	0.606389	0.492526	0.218237	0.225495	0.291932	0.271515	0.237173	0.281784	0.257786
Iso-05	0.705453	0.677779	0.457691	0.359112	0.544889	0.430544	0.439531	0.516171	0.453563	0.396119
Iso-06	0.606736	0.422822	0.400923	0.351216	0.375366	0.361049	0.32929	0.321007	0.292137	0.318042
Iso-07	0.649942	0.651781	0.623762	0.623034	0.639909	0.464699	0.225289	0.219731	0.250955	0.3424
Iso-08	0.770772	0.614863	0.5281	0.327084	0.188408	0.215324	0.248173	0.242243	0.264178	0.258138
Iso-09	0.745023	0.679602	0.516286	0.551967	0.60212	0.547318	0.534397	0.523138	0.442113	0.438931
Iso-10	0.682728	0.62896	0.609579	0.374676	0.328768	0.297518	0.267572	0.235619	0.289276	0.329628
Enf-01	0.717534	0.723738	0.660926	0.546588	0.426491	0.288177	0.311193	0.385414	0.422615	0.485991
Enf-02	0.600321	0.404382	0.375737	0.424702	0.443001	0.415924	0.447971	0.465681	0.460097	0.406184
Enf-03	0.531233	0.576416	0.335309	0.19716	0.202522	0.227774	0.257508	0.321101	0.344167	0.362232
Enf-04	0.765703	0.620539	0.492355	0.28632	0.168492	0.214412	0.24075	0.211609	0.187674	0.221962
Enf-05	0.572695	0.535491	0.401022	0.334509	0.336435	0.307602	0.319179	0.335237	0.325309	0.327527
Enf-06	0.503582	0.406577	0.450085	0.420845	0.411436	0.412036	0.406986	0.370103	0.411651	0.445861
Enf-07	0.532502	0.518669	0.507854	0.451757	0.493164	0.416277	0.280079	0.274419	0.303553	0.294224
Enf-08	0.682265	0.595385	0.457385	0.403076	0.352322	0.312621	0.31423	0.222915	0.224516	0.23655
Enf-09	0.70515	0.731499	0.576043	0.497984	0.455496	0.329483	0.319908	0.306684	0.325026	0.324227
Enf-10	0.589421	0.529481	0.426854	0.36702	0.416705	0.486401	0.341717	0.424236	0.283022	0.321246

Table 9-2 Tabular results of the non-linear forecasting for the measured time series

9.5.2 Graphical results of the nonlinear forecasting

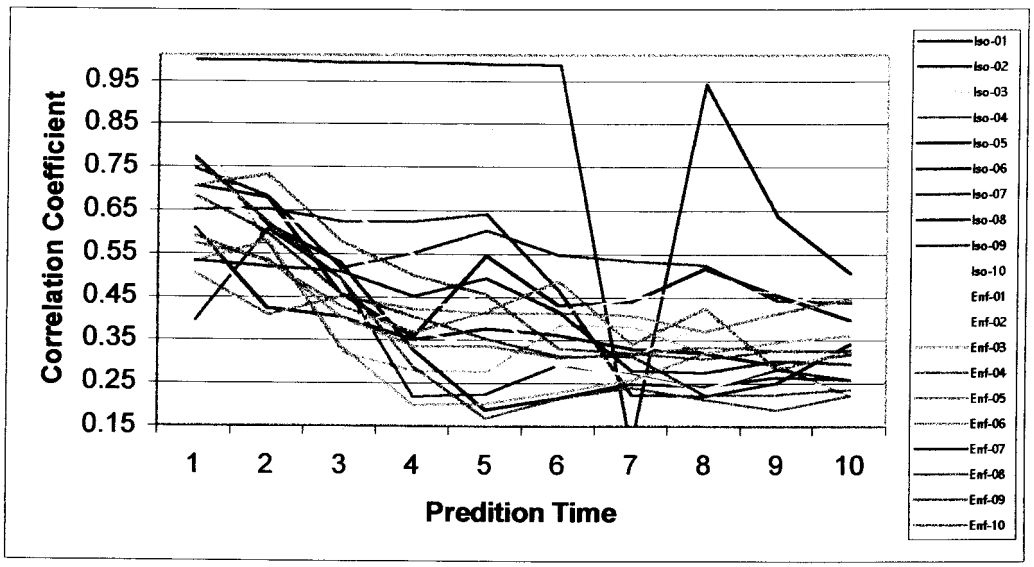

Figure 9-2 Graphical results of non-linear forecasting with all the measured time series

9.5.3 Individual Graphical Results with Noise as a control

Individual graphs of Non-Linear forecasting with a noise signal as control are to be found in Appendix I.

9.6 Statistical Analysis

The hypothesis and null hypothesis were formulated and stated in chapter 3, and are repeated here for clarity sake.

9.6.1 Hypothesis

The absorption of isoflurane and enflurane is a non-linear process. To detect nonlinearity four conditions must be met:

- Fractal Dimension of the attractor
- Sensitivity to initial conditions

- Invariant probability distribution of the attractor
- Detection of an underlying dynamical process

9.6.1.1 Null hypothesis

The absorption of the anaesthetic agents Isoflurane and Enflurane is fully described by independent and identically distributed random variables, i.e. the variability seen in the absorption is random[7] and there is no underlying deterministic process.

The time series measured will be analytically indistinguishable from noise signals.

9.6.1.2 Detection of an underlying dynamical process

This part of the hypothesis is being tested by this chapter.

9.6.2 Statistical Analysis of the Results

No recommendation is made by Sugihara et al1 on how to decide whether the time series under consideration is non-linear as determined by the method of Non-Linear forecasting other than graphical representation and imperial decision. Using this method, only one of the time series was considered not to demonstrate characteristics of a non-linear time series, namely Enf-016.

To make the decision more objective and less imperial, it was decided to calculate the coefficient of determination between the measured signal and the noise signal, using the values obtained with the Henon time series as a guideline for a coefficient of determination value which should be used in deciding if the time series should be considered non-linear or not.

SERIES	COEFFICIENT OF DETERMINATION	<<0.5	<<0.37	VISUAL
Henon	0.363	Yes	Yes	Yes
Io-01	0.263	Yes	Yes	Yes
Iso-02	0.082	Yes	Yes	Yes
Iso-03	0.281	Yes	Yes	Yes
Iso-04	0.151	Yes	Yes	Yes
Iso-05	0.281	Yes	Yes	Yes
Iso-06	0.446	Yes	No	Yes
Iso-07	0.169	Yes	Yes	Yes
Iso-08	0.234	Yes	Yes	Yes
Iso-09	0.331	Yes	Yes	Yes
Iso-10	0.246	Yes	Yes	Yes
Enf-01	0.091	Yes	Yes	Yes
Enf-02	0.169	Yes	Yes	Yes
Enf-03	0.055	Yes	Yes	Yes
Enf-04	0.277	Yes	Yes	Yes
Enf-05	0.198	Yes	Yes	Yes
Enf-06	0.156	Yes	Yes	No
Enf-07	0.256	Yes	Yes	Yes
Enf-08	0.250	Yes	Yes	Yes
Enf-09	0.168	Yes	Yes	Yes
Enf-10	0.342	Yes	Yes	Yes

Table 9-3 Statistical and visual analysis of non-linear forecasting on the henon and measured time series

The coefficient of determination for the Henon Time Series was calculated to be 0.363. The coefficient's of determination for the measured time series were all less than 0.5, and only one, Iso-06 is not less than 0.37. Adopting the most strict approach, that the nonlinear forecasting of a time series must not only visually be judged to be in favor of a nonlinear process, but also that the coefficient of determination be less than the control value, namely 0.37, the following is then deducted: nine out of the ten measured isoflurane time series and nine out of the ten measured enflurane time series are in favor of their being an underlying dynamical process in the absorption of the two gases. Is this statistically significant?

9.6.3 Testing for statistical significance

The problem identified in the section above will be statistically addressed using a binomial distribution[8].

9.6.3.1 Hypothesis and Null hypothesis

The hypothesis to be tested is as follows:H_1: $\pi > \pi_0$, with the null hypothesis being: H_0 : $\pi = \pi_0$. The value used for π_0 will be 0.5[8].

9.6.3.2 Power Analysis

To prevent a type II statistical error from being made, where the null hypothesis is accepted when the hypothesis is actually true, a power analysis[8] was performed. For the analysis, an alpha level of 1.645 was used which corresponds to a p value of < 0.05 for the rejection of the null hypothesis. A power level of >0.8 was considered acceptable[8].

9.6.3.2.1 Power Analysis for the Isoflurane Group

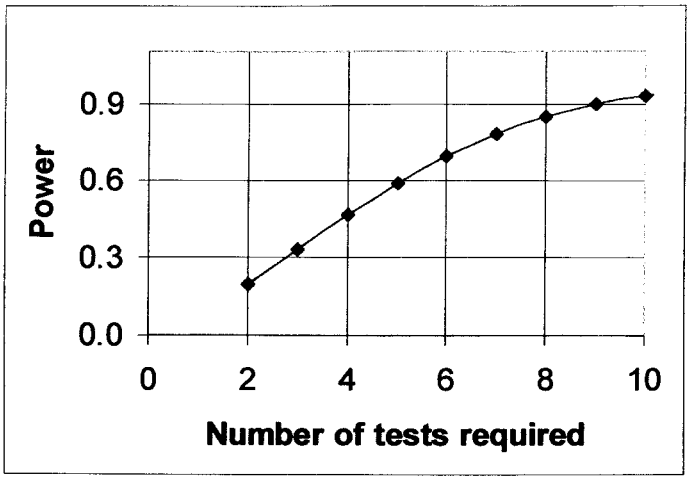

Figure 9-3 Power of the binomial for the isoflurane measured time series

9.6.3.2.2 Power Analysis for the Enflurane Group

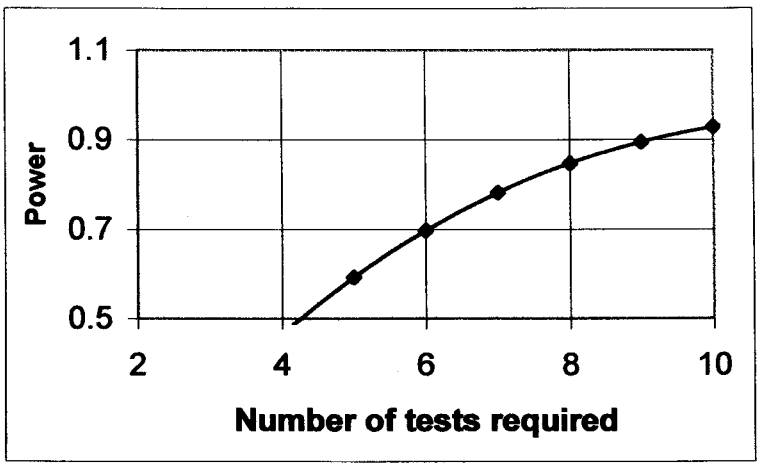

Figure 9-4 Power of the binomial for the enflurane measured time series

9.6.3.2.3 Power Analysis Conclusion

Ten binomial comparisons were used in each group. Both the power analysis showed that this was adequate for a power of > 0.8 and a p value of <0.05.

9.6.3.3 Results

	BINOMIAL RESULTS (P VALUES)
Isoflurane Group	0.01074
Enflurane group	0.01074

Table 9-4 Results of the binomial comparison

Both of the binomial comparisons yielded p values < 0.05. These results strongly recommend the acceptance of the hypothesis stated above (9.6.1) and more specifically, that there is evidence for an underlying dynamical process underlying the measured time series for both isoflurane and enflurane.

9.7 Conclusion

The results presented above show that there is evidence for a fractal attractor underlying the absorption of both isoflurane and enflurane using the method of nonlinear forecasting. These results reach statistical significance ($p < 0.05$) with acceptable statistical power (>0.8).

9.8 References

[1] Sugihara G.,May R.M. Nonlinear Forecasting As A Way Of Distinguishing Chaos From Measurement Error In A Time Series. Nature 1990:344;734-741.

[2] Lippman N.,Stein K.M.,Lerman B.B. Nonlinear Forecasting And The Daynamics Of Cardiac Rhythm. Journal Of Electrocardiology 1995:28;Supplement 65-70.

[3] Gong Y.,Xu J.,Ren W.,Hu S., Wang F. Determining The Degree Of Chaos From Analysis Of ISI Time Series In The Nervous System: A Comparison Between Correlation Dimension And Nonlinear Forecasting Methods. Biological Cybernetics 1998:2;159-165.

[4] Mansier P.,Clairambault J.,Charlotte N.,Medigue C.,Vermeiren C.,Lepape G.,Carre F.,Gounaropoulou A.,Swynghedauw B. Linear And Nonlinear Analyses Of Heart Rate Variability: A Minireview. Cardiovascular Research 1996:31;171-179.

[5] Aftans L.I., Lotova N.V.,Koshkarov V.I.,Popov S.A.,Mkhnew V.P. Nonlinear Forecasting Measurement Of The Human EEG During Evoked Emotions. Brain Topography 1997:10;155-162.

[6] Lui W.M. Nonlinear Forecasting Of Hepatitis And AIDS Incidence. Bulletin Of Mathematical Biology 1994:56;863-873.

[7] Cerutti S.,Carrault G.,Cluitmans P.J.M.,Kinie A.,Lipping T.,Nikolaidis N.,Pitas I., Signorini M.G. Non-Linear Algorithms For Processing Biological Signals. Computer Methods And Programs In Biomedicine 1996:51;51-73.

[8] Steyn A.G.W.,Smit C.F.,Du Toit S.H.C., Strasheim C. Modern Statistics In Practice. JL Van Schaik 1996

10 Statistical Analysis Summary

10.1 Hypothesis

The absorption of isoflurane and enflurane is a non-linear process. To detect non-linearity, four conditions must be met[1,2]:

1. Sensitivity to initial conditions
2. Fractal Dimension of the attractor
3. Invariant probability distribution of the attractor
4. Detection of an underlying dynamical process

10.2 Null hypothesis

The absorption of the anaesthetic agents Isoflurane and Enflurane is fully described by independent and identically distributed random variables, i.e. the variability seen in the absorption is random[3] and there is no underlying deterministic process.

The time series measured will be analytically indistinguishable from noise signals.

10.3 Testing the hypothesis

10.3.1 Method

Ten measured time series for both isoflurane and enflurane absorption were measured. These were then compared to ten noise signals, with similar standard deviations, means and number of points in the series.

10.3.2 Sensitivity to initial conditions

Calculating Lyapunov exponents tests for sensitivity to initial conditions.

STUDENT'S T-TEST RESULTS (P VALUE) FOR THE MEASURED TIME SERIES COMPARED TO NOISE CONTROLS	
Isoflurane group	0.000426 (power: 0.998495)
Enflurane group	0.000824 (power: 0.999492)

Table 10-1 Student's T-test (p value) for the measured time series compared to noise controls (Lyapunov exponent)

10.3.3 Fractal Dimension of the attractor

The dimension of the attractor was calculated using the following statistics. Each statistic gives an approximation of the fractal dimension. The approximate entropy is the only method described specifically for short, noisy, biological signals[4]. Therefore only the statistics calculated for the approximate entropy will be used for testing against the null hypothesis.

- Approximate entropy
- Information entropy
- Correlation dimension
- Fractal dimension (Box counting method)

STUDENT'S T-TEST RESULTS (P VALUES) FOR THE MEASURED TIME SERIES COMPARED TO NOISE CONTROLS				
	Approximate Entropy	Information Dimension	Correlation dimension	Fractal Dimension
Isoflurane group	0.000499 (Power: →1)	0.005435 (Power: 0.999905)	<0.000000 (Power: →1)	0.2133 (Power: 0.975885)
Enflurane group	0.003085 (Power: 0.999997)	0.028838% (Power: 0.999954)	0.000003 (Power: →1)	0.038049 (Power: 0.999427)

Table 10-2 Student's T-test (p values) for the measured time series compared to noise controls (fractal dimension)

10.3.4 Invariant probability distribution of attractor

Non linear forecasting was used to determine this characteristic. Each series was judged by a combination of visual and statistical criteria and then designated a "yes" or "no" answer. The proportions were analyzed using a binomial distribution, with $H_0 \pi$=0.5.

THE P VALUES OF THE BINOMIAL FOR THE 10 TESTS IN EACH GROUP		
Isoflurane group	0.01074 (Power: 0.928)	9/10 tests "yes"
Enflurane group	0.01074 (Power: 0.928)	9/10 tests "yes"

Table 10-3 The p values of the binomial for the ten tests in each group

10.3.5 Detection of an underlying dynamical process

This was determined by the method of surrogate data.

THE P VALUES FOR THE MEASURED TIME SERIES AND THEIR SURROGATES USING LYAPUNOV EXPONENTS AND CORRELATION DIMENSION AS COMPARISONS		
	Lyapunov Exponent group	Correlation Dimension Group
Isoflurane group	0.0378105 (Power: →1)	0.0000001 (Power: →1)
Enflurane group	0.0000119 (Power: →1)	0.0000187 (Power: →1)

Table 10-4 The p values for the measured time series and their surrogates using Lyapunov exponents and correlation dimension as comparisons

10.4 Conclusion

Each of the four conditions required by the hypothesis have been met with statistical significance ($p < 0.05$) and acceptable statistical power (>0.8). It is therefore concluded that the null hypothesis should be rejected and accepted that the absorption of both isoflurane and enflurane are non-linear processes.

10.5 References

[1] Moon F.C. Chaotic And Fractal Dynamics: An Introduction For Applied Scientists And Engineers. John Wiley And Sons1992

[2] Bassingthwaighte J.B.,Liebovitch L.S.,Westb.J. Fractal Physiology. Oxford Universtity Press 1994.

[3] Cerutti S.,Carrault G.,Cluitmans P.J.M.,Kinie A.,Lipping T.,Nikolaidis N.,Pitas I., Signorini M.G. Non-Linear Algorithms For Processing Biological Signals. Computer Methods And Programs In Biomedicine 1996:51;51-73.

[4] Pincus S.M.,Goldberger A.L., Physiological Time-Series Analysis: What Does Regulatory Quantify? American Journal Of Physiology 1994:266;H1643-H1656

11 Discussion

11.1 Implications for anaesthesia

11.1.1 Administration

11.1.1.1 User adjusted inhalation agent concentration

The practice whereby the anaesthesiologist adjusts the concentration of the inhalation agent against the patient's response to stimuli does not require any change, because this process is inherently non-linear.

11.1.1.2 Calculated inhalation agent concentration

The method of pre-calculated injections described by Lowe[1] assumes that the absorption of the inhalation agent is predictable and therefore needs to be adjusted or phased out.

Computer assisted anaesthesia provision where preset concentrations are entered by the user are coming into practice, for example, Dräger's "Physioflex." These types of anaesthesia machines can compensate for a nonlinear absorption, provided that a feedback loop is built into the system, allowing adjustment of the inspired concentration based on the expired concentration of inhalation agent.

11.1.2 Modelling

Prediction is the sine qui non of modelling[2] and studying biological signals is the first step toward this end. Presently prediction of how non-linear systems behave in the real world is only possible for a limited period of time[3]. As further mathematical techniques are developed and the dynamics underlying non-linear processes are further discovered, this goal should be realized. For the moment, it eludes us.

11.1.3 Pharmacokinetics

Standard textbooks do not mention pharmacokinetic models other than those based on compartments described by single or multiple exponential equations. Non compartmental models, which have kinetics, that are fractal in nature, have been described for tracers[4], ^{15}O-labeled Water,[5] and opiates[4].

If the non-linear nature of inhalation agent absorption is taken into account when simplified models are described, then the search for an ideal model that accurately describes the process will prove to be futile. Maybe the 40 odd years since Severinghaus and the square root of time model have proved this!

11.2 Literature evidence against the compartmental models

11.2.1 Assumptions made in linear modeling

11.2.1.1 Assumptions made in the compartment model

A compartment is a region or subspace within a biological system throughout which the concentration of some substance is regarded as uniform[4]. A compartmental model is one consisting of one or several of such subspaces. The rate of exchange of material between compartments is governed by a set of non-negative rate coefficients, which are usually taken to be constant in time. Not every compartment in a given system exchanges material with every other compartment, which allows compartmental models to assume various configurations such as the catenary or linear model, and the radially symmetric or mammillary model[4].

Compartments are largely intuitive structures and they can be useful for both heuristic and computational purposes. They are governed by sets of ordinary differential equations, where time is the sole independent variable, and the concentrations or masses of material in the various compartments are the dependent variables. One differential equation can be written for each compartment to govern the flow of material to and from this

compartment. Compartments are easily visualized and sometimes identifiable with anatomical spaces[4].

In a steady state, the amount of substance within a compartment remains constant. When the steady state is displaced by means of a disturbance that increases or decreases the amount of material in one or more compartments, the masses of material in many of the compartments will change with time. When the disturbance is removed, the system will return to steady state. This relaxation process, under the influence of constant rate coefficients, will be described by sums of real, negative exponential functions. The real negative exponential is the characterizing function of the linear compartmental model, although complex exponents giving rise to sine and cosine terms, can, in principle appear[4].

When the clearance of a substance is measured by some or other means, a clearance curve can be constructed. When such a process is modeled by means of a linear compartmental model, one compartment of which contains the plasma; the mathematical function governing the clearance curve will consist of sums of real, negative exponentials. If the logarithm of the plasma concentration of the substance under consideration is plotted against time, and if a compartmental model is a valid representation of the biokinetic process of plasma clearance, data will tend to fall on a straight line for large values of time. Stated otherwise, a semi-log plot of clearance data will tend to approach linearity with increasing time[4].

11.2.1.2 The System Model for Closed-circuit Inhalation Anaesthesia

This model is the most recently described compartmental model of inhalation anesthetic agents in the literature[6].

It does not assume a constant alveolar concentration of inhalation agent, and therefore lends itself to validation by non-invasive measuring techniques as well as attempting to predict the breath by breath alveolar concentration after bolus injections of liquid inhalation agent.

The basic model for the uptake and distribution of a single inhalation anesthetic depicts the body and the closed circuit as a system of 14 compartments. The anesthetic agent is taken up from the lung-closed circuit compartment and is then distributed to the other tissue compartments: kidney, brain, liver, muscle, connective tissue, and adipose tissue. The model derives from the subject's age, body weight, height and gender the other physiological variables, including tissue volumes, blood volume, cardiac output, dead space, alveolar space and tidal volume[6]. This type of model has been illustrated by both hydraulic[7] and electrical[8] analogies.

The data source for the total blood volume, cardiac output, tissue volumes, tissue blood flows, and partitian coefficients were based on that of Lowe[1].

Two extensions were made to the basic model to include the effect of the anesthetic agent on cardiac output and to allow monitoring feedback from expiratory gas[6].

11.2.2 Shortfalls in the compartmental model noted in the literature to date

11.2.2.1 Failure to recognize the functional residual capacity as an extension of the anaesthetic circuit

This criticism has been leveled by Lin[9] against both the square root of time model and the compartmental models such as those described by Lerou et al[6]. The basis of this argument is that the functional residual capacity must be considered part of the breathing circuit and not as part of the "lung compartment" as done by both the examples mentioned. This criticism by Lin is backed up by experimental evidence[10] where the absorption of nitrous oxide was determined by a subtraction method. Their results differ significantly from those previously described, showing that the initial absorption of nitrous oxide was minimal and that after a period of functional residual capacity washin, the absorption was relatively constant[9].

11.2.2.2 Failure to recognize the alveolar membrane as a barrier

The mathematical model of uptake described by Eger[11] used the Fick principle in part to explain the uptake of anesthetic agents, but only took the solubility coefficient and the partial pressure across the membrane to explain uptake, but did not include the diffusion coefficient, the area of the membrane or the thickness of the membrane into account. This is again pointed out by Lin[9], who then proposes that the absorption of anaesthetic agents should be represented by 1-(Alveolar fraction/Inspired fraction) and not by the (Alveolar fraction/Inspired fraction) as proposed by Eger[11]. The method of Lin's was used in this thesis to calculate the absorption of anesthetic agents.

Anaesthetic uptake has been traditionally described using high flow techniques during which the inspired concentration is held constant[9]. The relationship between the alveolar (Fa) and inspired (Fi) concentrations over time (Fa/Fi curve) is used to describe the pharmacokinetics. However, several misconceptions exist regarding the meaning of the Fa/Fi curves. The initial portion of the Fa/Fi curves represents mostly washin of the anaesthetic circuit and the functional residual capacity, and patient uptake is probably minimal during the first few minutes of an anaesthetic[12]. In addition, the Fa/Fi curves by themselves do not describe the patient uptake, but uptake is rather represented by the area above the Fa/Fi curves and is the product of Fi, the fraction of uptake (1-Fa/Fi) and the alveolar ventilation[9].

11.2.2.3 No correlation with patient demographics

In a study designed to see whether patient characteristics (age, height, weight, body surface area, and cardiac output estimated by the Brody formula) could predict the uptake of desflurane and isoflurane[12], the authors conclude, "There was a poor correlation between uptake and patient characteristics. Interindividual variability in the uptake is likely not as a

result of patient characteristics." Other studies have reached similar conclusions[14,13]

11.2.2.4 Failure to describe adequately statistical methods

Two articles recently describe the absorption of isoflurane and desflurane during anesthesia[14,15]. A tri-exponential and bi-exponential model were fitted respectively. However, almost no statistical information is given. This forces one to regard these results with caution.

11.2.2.5 Fractal nature of structure and blood flow of organs

Organs are not normally homogeneously perfused[5]. Regional blood flows in the heart are broadly heterogeneous. In both the heart and lung, the spatial variation appears to be fractal. This means that the spatial heterogeneity shows statistical self-similarity. Fractal like anatomy has been described for the arterial and venous trees, the branching of cardiac muscle bundles, the tracheobronchial tree, and the His-Purkinje network[16]. Other organ systems containing fractal like structures including the nervous system, the bowels, the billiary duct system, and the renal calyces[16].

11.2.2.6 Fractal nature of flow limited blood-tissue exchange and the invalidity of the "well stirred" tank model

Bassinghtwaighte et al[5] measured flow-limited washout of a tracer from the heart. The data exhibited a particular combination of power law forms. The interpretation is that both the residue and the outflow curves demonstrate self-similarity, in the sense that for each proportional increase in time, there is a constant proportional diminution in signal. In the field of nonlinear dynamics, this is termed power law behavior. Such behavior is the hallmark of fractals, the self-similarity means that apparent behavior is independent of the time unit considered. The evidence points strongly to the conclusion that the myocardial water washout is a fractal process.

The observed fractal washout may be explicable on the basis that regional flows per gram of tissue have spatial distributions[5].

This study contrasts notably with and clearly refutes, the long held perception that washout is an exponential prosess.[5]

11.2.3 Alternatives to the compartmental model

Compartmental models remain the most popular means of modeling kinetic data in the medical literature at present, but they are not used universally[4]. Non-compartmental models are defined as those models that do not necessarily require the presence of regions that are well mixed. Concentrations of drugs may vary continuously both in space and time within the organism. Continuous concentration gradients will be permitted. Partial differential equations or integral equations may replace the ordinary differential equations of compartmental systems[4].

The power function given by $C = At^{-\alpha}$ is proposed as an alternative. The clearances of both drugs and tracers have been modeled using this function[4]. One area of great theoretical interest involves the area of its application, in that the concept of biological halftime is completely fallacious and may result in gross errors, both actually and conceptually.

The power function may arise from the diffusion process, which constitute a rate-limiting step for removal of certain substances from the circulation (see 11.2.2.2). It has been realized for some time that a power function can be related to the sum or integral of an infinitely large number of exponential functions[4].

11.2.4 The role of statistical tests

When measured data can be curve fitted by a power function requiring only two or three adjustable parameters and gives rise to a smaller sum of squares residuals than required by a curve, for example a triple exponential with six adjustable parameters, the case for the power function would seem overwhelming[4]. It is probably true that statistical tests in

themselves convince us that one model is to be preferred over another, but there are circumstances where no intuitive or geometric criteria really present themselves. One may then seek refuge in purely statistical criteria[4]. One wonders whether functions are decided upon merely because it was assumed that it should be so, when another function would fit the data equally well[17].

11.3 Possible sources of non linearity in the absorption process

11.3.1 Non-heterogeneous blood flow

The standard textbook lists the flows of blood to organs in ml/min or in ml/g/min.[18] No indication of intra-organ variation will be found, and the ranges of values given implicitly reflect with inter-animal or temporal fluctuation. For years, there was a generally held opinion that the variation in apparent regional blood flow was due to unavoidable experimental errors in the methods used. Recently it has been shown that the spatial dispersion of the heterogeneity of blood flow in the heart has a fractal dimension approaching 1.2, and for the lung of approximately 1.1[18]. These values are very similar to the information dimension values calculated for the measured time series of isoflurane and enflurane. The values were 1.12 and 1.29 respectively.

11.3.2 Fractal vascular anatomy

The dichotomously branching and randomly asymmetric variation models of simple bifurcating networks of blood vessels that have been described[18], prove adequate to describe the dependence of the relative dispersion of the flow distribution on the size of the supplied region, even though they give overly simple descriptions of the vascular network. In each case, the form of the microvascular network is linked to an experimentally measurable variable, local blood flow, and its heterogeneity in the normally functioning organ. While this approach has been tried only in the heart and lung, it seems safe to predict that such fractal approaches

will be useful in describing other systems with heterogeneous flow distributions[18].

11.3.3 Dynamic state of the cell membranes in the body

The compartment model of inhalation agent absorption ignored membranes and used solubility coefficients derived from cadaver specimens of organs[6]. This meant that any dynamic from either heterogeneity of blood flow or of the membranes themselves were ignored or never considered. It is now proven that the membranes in the absorption process constitute a barrier to the absorption process[9]. Chaotic models of cell membrane channel kinetics have been proposed in the recent literature[18] and could partly explain variability in cell membrane permeability over time. Other mechanisms cannot be excluded.

11.3.4 Physiological advantages of chaos

Chaotic systems can be controlled more finely and more quickly than linear systems. In linear systems, the response of the output depends linearly on the input. Small changes in a parameter of a linear system produce only small changes in output. Chaotic systems can have bifurcations, and qualitative changes in behavior as a parameter is varied. Thus, small changes in a parameter of a chaotic system can produce very large changes in the output. Hence, a chaotic system is under much finer control. The variable controlling a chaotic physiological response may need to change only a small amount to induce the desired large change in the physiological state. A chaotic physiological system can switch very quickly from one state to another[18].

"Homeostasis," the stability of the "milieu interieure" has been regarded as the modus operandi of physiological systems since the time of Claude Bernard. The principle was that the body is designed so that the concentrations and rates of processes tended toward a stable state, through multiple feedback mechanisms. This was not a passing idea, for it had many affirmations and was firmly positioned in the medical literature. Now

the questions is posed if the term homeostasis should not be replaced by the term homeodynamics, allowing a more flexible view of how the systems work and making room for the concept of systems with complex responses, even to the point of instability[18].

11.4 Why were only two gases used?

11.4.1 Are these results necessarily applicable to other gases used in anaesthesia?

In the anaesthesia literature, inhalation agents are treated as a homogenous group as far as pharmacokinetics are concerned, with two notable exceptions, halothane, and methoxyflurane.[8] The unity of the group originates in the different solubilities of the agents predicting minimum alveolar concentrations at which responses to noxious stimuli are blunted. The two exceptions are made because they are the only two agents that are metabolized to a significant degree in the body, affecting their kinetics. Due to cost and time constraints, two of the most commonly used inhalation agents in South Africa were chosen as examples for this thesis.

11.5 References

[1] Altrete J.A., Lowe H.J., Virtue R.W. Low Flow And Closed System Anesthesia. Grune And Stratton 1979.

[2] Sugihara G.,May R.M. Nonlinear Forecasting As A Way Of Distinguishing Chaos From Measurement Error In Time Series. Nature 1990:344;734-741.

[3] Pietgen H.,Jurgens H.,Saupe D. Chaos And Fractals New Frontiers Of Science. Springer-Verlag 1992.

[4] Norwhich K.H. Noncompartmental Models Of Whole Body Clearance Of Tracers: A Review. Annals Of Biomedical Engineering 1997:25;421-439

[5] Bassingthwaighte J.B., Beard D.A. Fractal ^{15}O-Labeled Water Washout From The Heart. Circulatory Research 1995:77;1212-1221

[6] Lerou J.G.C.,Dirksen R,Beneken Kolmer H.H.,Booij L.H.D.J. A System Model For Closed-Circuit Inhalation Anaesthesia. Anesthesiology 1991:75;345-355

[7] Coetzee J.F. Are Target-Controlled Infusions A Real Advance? Refresher Course In Anaesthesia, University Of Natal, Department Of Anaesthesia 1998.

[8] Mapleson W.W. Pharmacokinetics Of Inhaled Anaesthetics. In Prys Roberts C., Hug C.C., (Editors). Pharmacokinetics For Anaesthesia Blackwell Scientific Publications 1984, Pp89-111.

[9] Lin C.Y. Uptake Of Anaesthetic Gases And Vapours. Anaesthesia And Intensive Care 1994:22;363-373.

[10] Lin C.Y., Mostert J.W., Benson D.W. Closed Circle Systems-A New Direction In The Practice Of Anesthesia. Acta Anaesthesia Scandinava 1980:24;354-361.

[11] Eger EI II. Application Of A Mathematical Model Of Gas Uptake. In: Papper E.M.,Kitz R.J., Eds. Uptake And Distribution Of Anesthetic Agents. Mcgraw-Hill, New York 1963: Ch 8, Pp 88-103.

[12] Hendrickx J.F.A.,Soetens M,Van Der Donck A,Meeuwins H,Smolders F, De Wolf A.M. Uptake Of Desflurane And Isoflurane During Closed Circuit Anaesthesia With Spontaneous And Controlled Mechanical Ventilation. Anaesthesia And Analgesia 1997:84;413-418

[13] Westenskow D.R., Jordan W.S., Hayes J.K. Uptake Of Enflurane: A Study Of The Variability Between Patients. British Journal Of Anaesthesia 1983:55;595-601

[14] Lockwood G.G.,Chakrabarti M.K., Whitwam J.G. The Uptake Of Isoflurane During Anaesthesia. Anaesthesia 1993:48;748-752.

[15] Walker T.J., Chakrababarti M.K.,Lockwood G.G. Uptake Of Desflurane During Anaesthesia. Anaesthesia 1996:51;33-36

[16] Godlberger A.L. Non-Linear Dynamics For Clinicians:Chaos Theory, Fractals And Complexity At The Bedside. The Lancet 1996:347;1312-1314.

[17] Steyn J.D. Context Sensitive Decrement Times Of Inhaled Anesthetics And The Power Function. SASA 99 Congress Presentation, In Press.

[18] Bassinghtwaighte J.B.,Liebovitch L.S.,West B.J. Fractal Physiology, Oxford University Press 1994.

12 Conclusion and Implementation

12.1 Conclusion

The results presented in this thesis meet the four conditions required to accept the hypothesis that the absorption of both isoflurane and enflurane are non linear, with statistical significance ($p<0.05$) acceptable statistical power ($p>0.8$). The four conditions met are: sensitivity to initial conditions, fractal dimension of the attractor, invariant probability distribution of the attractor and detection of an underlying dynamical process.

It is therefore concluded that the absorption of the anaesthetic agents isoflurane and enflurane is non linear.

12.2 Implementation in Anaesthesia practice

12.2.1 Anaesthesia Administration

12.2.1.1 User adjusted inhalation agent concentration

The practice whereby the anaesthesiologist adjusts the concentration of the inhalation agent against the patient's response to stimuli does not require any change, because this process is inherently non-linear.

12.2.1.2 Calculated inhalation agent concentration

The method of pre-calculated injections described by Lowe[1] assumes that the absorption of the inhalation agent is predictable and therefore needs to be adjusted or phased out.

Computer assisted anaesthesia provision where preset concentrations are entered by the user are coming into practice, for example, Dräger's

"Physioflex." These types of anaesthesia machines can compensate for a nonlinear absorption, provided that a feedback loop is built into the system, allowing adjustment of the inspired concentration based on the expired concentration of inhalation agent.

12.2.2 Anaesthesia Modelling

Prediction is the sine qui non of modelling[2] and studying biological signals is the first step toward this end. Presently prediction of how non-linear systems behave in the real world is only possible for a limited period of time[3]. As further mathematical techniques are developed and the dynamics underlying non-linear processes are further discovered, this goal should be realized. For the moment, it eludes us.

12.2.3 Anaesthesia Pharmacokinetics

Standard textbooks do not mention pharmacokinetic models other than those based on compartments described by single or multiple exponential equations. Non compartmental models, which have kinetics, that are fractal in nature, have been described for tracers[4], ^{15}O-labeled Water,[5] and opiates[4].

If the non-linear nature of inhalation agent absorption is taken into account when simplified models are described, then the search for an ideal model that accurately describes the process will prove to be futile. Maybe the 40 odd years since Severinghaus and the square root of time model have proved this!

12.3 References

[1] Altrete J.A., Lowe H.J., Virtue R.W. Low Flow And Closed System Anesthesia. Grune And Stratton 1979.

[2] Sugihara G.,May R.M. Nonlinear Forecasting As A Way Of Distinguishing Chaos From Measurement Error In Time Series. Nature 1990:344;734-741.

[3] Pietgen H.,Jurgens H.,Saupe D. Chaos And Fractals New Frontiers Of Science. Springer-Verlag 1992.

[4] Norwhich K.H. Noncompartmental Models Of Whole Body Clearance Of Tracers: A Review. Annals Of Biomedical Engineering 1997:25;421-439

[5] Bassingthwaighte J.B., Beard D.A. Fractal ^{15}O-Labeled Water Washout From The Heart. Circulatory Research 1995:77;1212-1221